AFCRL-63-69

Investigation of VARIOUS ACTIVATOR REFRACTORY SUBSTRATE COMBINATIONS

J. H. Affleck

Power Tube Department
General Electric Company
Schenectady 5, New York

Contract No. AF 19(628)-279
Project No. 4619
Task No. 46190!

Final Report
March 5, 1963

Prepared
for

ELECTRONICS RESEARCH DIRECTORATE
AIR FORCE CAMBRIDGE RESEARCH LABORATORIES
OFFICE OF AEROSPACE RESEARCH
UNITED STATES AIR FORCE
BEDFORD, MASSACHUSETTS

Requests for additional copies by Agencies of the Department of Defense, the contractors, and other Government agencies should be directed to the:

ARMED SERVICES TECHNICAL INFORMATION AGENCY
ARLINGTON HALL STATION
ARLINGTON 12, VIRGINIA

Department of Defense contractors must be established for ASTIA services or have their "need-to-know" certified by the cognizant military agency of their project or contractor.

All other persons and organizations should apply to the:

U.S. DEPARTMENT OF COMMERCE
OFFICE OF TECHNICAL SERVICES
WASHINGTON 25, D. C.

AFCRL-63-69

Investigation of VARIOUS ACTIVATOR REFRACTORY SUBSTRATE COMBINATIONS

J. H. Affleck

Power Tube Department
General Electric Company
Schenectady 5, New York

Contract No. AF 19(628)-279
Project No. 4619
Task No. 461901

Final Report
March 5, 1963

Prepared
for

ELECTRONICS RESEARCH DIRECTORATE
AIR FORCE CAMBRIDGE RESEARCH LABORATORIES
OFFICE OF AEROSPACE RESEARCH
UNITED STATES AIR FORCE
BEDFORD, MASSACHUSETTS

FOREWORD

This report was prepared by Mr. John H. Affleck of the Power Tube Department of the General Electric Company, Schenectady, New York, on Air Force Contract No. AF19(628)-279, under Task No. 461901 of Project No. 4619. Work on the project was originated on July 1, 1958 on Air Force Contract No. AF19(604)-4093 and at the expiration of this contract on January 31, 1962 was continued on Air Force Contract No. AF19(628)-279 from February 1, 1962 through January 31, 1963. The research reported in this document was sponsored by the Electronics Research Directorate of the Air Force Cambridge Research Laboratories, Office of Aerospace Research, United States Air Force, Bedford, Massachusetts, with J. H. Bloom as contract monitor.

The following five patent applications were filed during the course of this investigation:

Patent Docket No. 36-62D-195, "Emitter and Method of Making," J. H. Affleck.
Patent Docket No. 36-62D-310, "Electron Emitter," J. H. Affleck and Dr. N. J. Hawkins.
Patent Docket No. 36-62D-343, "Thermionic Emitter and Method of Making Same," J. H. Affleck.
Patent Docket No. 36-62D-372, "Dispenser Cathode," J. H. Affleck.
Patent Docket No. 36-62D-373, "Dispenser Cathode," J. H. Affleck.

ABSTRACT

An investigation has been conducted under Air Force Contracts No. AF19(604)-4093 and No. AF19(628)-279 to study thin-film activator-refractory substrate combinations to produce new materials capable of producing high emission density cathodes.

Consideration is given to the nature of the boundary, the surface of the cathode, and vacuum in an externally dispensed system. Although a relation between the relative evaporation rate of electrons and the evaporation rate of the activator may be obtained, experimental confirmation in compliance with the basic assumptions is extremely difficult.

An empirical examination of internally dispensed systems has been made to show what effect the substrate has on the thermionic properties of a dispenser cathode. A number of systems are reported which combine a barium compound with a refractory material such as tungsten, tantalum, molybdenum, or one of the carbides, borides or silicides of these same elements. As a result of the determination of the thermionic constants and the evaporation rate of the activator, it appears that the activator-substrate combination has only a secondary effect on the thermionic properties in the system examined. This is attributed to the non-uniformity of the emitting surface and to the absence of exactly a monolayer coverage by the activator.

TABLE OF CONTENTS

LIST OF ILLUSTRATIONS

LIST OF TABLES

SECTION I
INTRODUCTION

It is generally appreciated that many, if not most, electron tubes are limited in life and performance by the cathode. An examination[1] of factors limiting frequency and power obtainable from electron tubes also reveals that cathode inadequacies are the most important of these limitations. In applications where high-current densities are required, the oxide-coated cathode has a number of basic limitations. Some of these limitations, along with properties necessary for a high-current emitter, are examined in APPENDIX I. Because of the limitations of the oxide-coated cathode and the desire for higher current densities and longer life, considerable effort has been expended to develop new cathodes. In general, this effort has been spent on systems known as thin-film emitters. The term "thin-film emitter" is usually defined as a cathode composed of a suitable conducting substrate whose surface is covered by a thin film of an electropositive element, the order of one atom thick, which results in a modified work function for the emitting surface.

There are a number of examples of this phenomena. Langmuir and Kingdon[2] found that an adsorbed layer of cesium-on-tungsten resulted in a lower work function of the tungsten, such that the thermionic emission at a temperature of 700°K increased by 21 orders of magnitude. By adding oxygen in such a way that the system consisted of cesium-on-oxygen-on-tungsten, the emission increased an additional three orders of magnitude. The maximum practical operating temperature also could be increased, since it was now possible to maintain a monolayer coverage at higher temperatures. However, the emission density of a cesium cathode is still impractically low in conventional electron tubes because of the high vapor pressure of cesium.

One system that has been found to be more practical is thorium-on-tungsten. Brattain and Becker[3] have shown the emission to be 10^6 greater than tungsten at 2000°K. By carburizing the tungsten, some additional improvement has been experienced in the emission efficiency.

Manuscript released by the author for publication on February 15, 1963.

Still another approach that has resulted in a low work function and improved efficiency is to add barium to tungsten. Improvement in emission by 10^{11} over tungsten is achieved and operating temperatures begin to approach the oxide cathode. By adding oxygen (i.e., W-O-Ba), the emission is improved by a factor of two over W-Ba.[4] A system of this general type is the basis for the L-cathode.[5,6]

It is clear that the emission is affected rather markedly in these "thin-film" systems. Additional benefits are gained from the introduction of an oxide or carbide layer between the base and the sorbed film. Questions are then raised as to what effect the substrate-activator combination has on the over-all work function and what are evaporation rates of the "activator" in the thin-film emitters.

The logical extension of investigations concerning thin-film emitters is to study the effect on various activator refractory substrates combinations on emission and evaporation characteristics. Therefore, the general objective of this study was to determine the principles that will permit the design of thermionic cathodes which possess the combined properties of high electron emission and long life. Specifically, the objectives were (1) to study experimentally the emission and evaporation rate of cathodes composed of refractory salts in conjunction with low work function activator elements and (2) to attempt to evolve a correlation theory which would not only aid in design of practical cathodes, but also give a better understanding of the mechanism of operation of thin-film emitters.

The investigation covered in this report is the result of two contracts sponsored by the Electronics Research Directorate of the Air Force Cambridge Research Center, Air Research and Development Command - Contract No. AF19(604)-4093 from July 1, 1958 through January 31, 1962 and Contract No. AF19(628)-279 from February 1, 1962 through January 31, 1963. Initial efforts consisted of dispensing the activator onto a refractory base from the vapor phase (i.e., external dispensing). Then, systems which contained the activator were examined (i.e., internal dispensing).

SECTION II
PHASE I - EXTERNAL DISPENSING

A. GENERAL CONSIDERATIONS

Vital to the design of cathodes by the dispenser principle is the nature of the boundary between the surface of the cathode and the vacuum, and the dynamics of what goes on there. This is the problem which had to be examined first.

I. Langmuir described experiments on the cesium-on-tungsten system in two monumental papers[7, 8] and produced a theory to explain nearly all of the observed results of evaporation and emission. A study of these papers indicates the distinct possibility that Langmuir has, in fact, outlined a general approach to the total problem of the nature of emitting surfaces in the case of materials to be studied in this program. The salient features, assumptions, and conclusions of this approach are discussed by Dr. N. J. Hawkins in APPENDIX II.

B. EXPERIMENTAL PROCEDURE

1. Methods of Emitter Evaluation

During Phase I, the experimental efforts of this study consisted of obtaining the thermionic constants of the refractory salts with and without activators. These parameters were needed for theoretical as well as practical considerations. The thermionic constants are defined by the Richardson-Dushman equation which states that:

$$I_o = A_o (1-r)\, T^2\, e^{-e\phi/kT} \qquad (1)$$

where
- I_o = zero field emission density
- A_o = 120 a/cm^2/deg^2
- r = reflection coefficient
- ϕ = effective work function
- e = electronic charge
- k = Boltzmann's constant
- T = cathode temperature in ^oK

However, ϕ varies linearly with temperature according to:

$$\phi = \phi_o + \alpha T \tag{2}$$

where ϕ_o = work function at absolute zero or the Richardson work function

α = $d\phi/dT$, the temperature coefficient of the work function.

Substituting Equation (2) into Equation (1):

$$I_o = A_o (1-r)\, T^2\, e^{-e\, \frac{(\phi_o + \alpha T)}{kT}} \tag{3}$$

or

$$I_o = A_o\, e^{-e\,\alpha/k}\, (1-r)\, T^2\, e^{-e\,\phi_o/kT} \tag{4}$$

If the term containing the reflection coefficient is neglected, then:

$$I_o = AT^2\, e^{-e\,\phi_o/kT} \tag{5}$$

where: $A = A_o\, e^{-e\alpha/k}$

This is the form of the Richardson-Dushman equation that is used in practice. Experimentally, a simultaneous measurement of I_o and T is made at various temperatures and plotted as the log I_o/T^2 versus $1/T$. This type of plot is called the "Richardson plot." The slope of the curve gives the Richardson work function, ϕ_o, and A is determined from Equation (5).

In order to measure ϕ and A, it is necessary to perform an experiment in which the zero field emission, I_o, can be determined as a function of temperature, T. It is not practical to measure emission currents at exactly zero field due to complications introduced by space charge, particularly at high temperatures. For this reason, the zero field emission current is usually obtained by extrapolating the measured emission current to the value at zero field from values obtained in either the retarding field or in the accelerating field regions.

In an accelerating field, the Schottky effect reduces the surface barrier at the cathode, and the emission current density is:

$$I = I_o e^{BE^{1/2}/T} \tag{6}$$

where E is the electric field at the cathode surface and B a constant. For either plane parallel or coaxial anode-cathode geometry, E is directly proportional to the applied accelerating voltage, V_a. By means of this relationship and the Schottky equation, I_o is obtained by an extrapolation of the measured currents to zero field.

In the retarding field case, the application of a negative voltage to the anode of a diode creates a potential barrier that retards all electrons with energy less than the potential minimum. In terms of zero field current density, I_o, the collected current in a plane parallel geometry is:

$$I_R = I_o e^{eV_R/kT} \tag{7}$$

where V_R is the true retarding voltage. The retarding voltage may differ from the applied anode-cathode voltage, V_a, by the contact potential existing between these two electrodes. I_o is determined from the intersection of the two straight line portions of the curve obtained by plotting the logarithm of the measured current, I_R, versus the applied voltage, V_a.

Both methods require a measurement of current and voltage at several temperatures in order to determine I_o as a function of temperature. The effective work function of the emitter then may be obtained by substituting values for I_o and T in Equation (1) assuming A_o = 120 $a/cm^2/deg^2$ and r = 0. In practice, rather than actually solving the equation for each ϕ, it is more convenient to use an effective work function chart as suggested by Hensley.[9] More accurate results may be obtained using the detailed graphs of Jansen and Loosjes.[10] These present the current density versus absolute temperature with lines of constant effective work function given for every 0.05 ev. Once the effective work function has been determined over a temperature, the temperature coefficient is readily determined and by extrapolating to 0^oK the Richardson work function, ϕ_o, is found. Thus having determined the constants ϕ_o and α, the effective work function of an emitter can be completely specified as a function of temperature in the form of Equation (2).

2. Experimental Results

The thermionic emission data was obtained in a test diode structure which consisted of a directly heated filament mounted in a cylindrical guard ring structure. A filamentary cathode was used in order to conveniently take measurements over a large temperature range and to easily heat the cathode to temperatures above 1500°K. However, one problem which arises when a filamentary cathode is used is that the cathode does not have a unipotential surface. This can be overcome by using half-wave rectified a-c for heating the cathode and by measuring the retarding field current only during the "off" cycle. The circuit used is shown in Figure 1. An optical pyrometer was used to measure the filament temperature with the appropriate corrections being made for the spectral emissivity.

Initial measurements were made using molybdenum and molybdenum silicide as filamentary cathodes. The effective work function of molybdenum was found to be 4.2 ev at a temperature of 1400°K, which agreed with the published data[11] and established the validity of the experimental technique. Measurements conducted on molybdenum silicide gave an effective work function of 4.7 ev at a temperature of 1650°K. Further tests indicated that this material probably could not be operated above 1750°K without excessive evaporation of silicon.

Although these values are of interest, the more important consideration is the amount by which the work function is lowered by the adsorption of an activator such as cesium or barium. Initial experiments were conducted using cesium as the activator on molybdenum and on molybdenum silicide. The object of these experiments was to determine the reduction of the work function and the relative evaporation rate of the activator from the substrate.

Tubes were constructed which consisted of a directly heated filament mounted in a cylindrical guard ring structure. All tubes were equipped with a barium getter which was flashed after the tubes were sealed off the vacuum station. A cesium generator was also included which consisted of a directly heated nickel tube filled with cesium chromate and silicon. By passing current through the nickel tubing, the cesium chromate is reduced by the silicon, producing cesium in the tube. Emission measurements were made using a retarding potential method to determine the zero field emission, I_o. The temperature of the filament was determined with the aid of an optical pyrometer and was correlated with other data that related the wire diameter, current, and temperature.

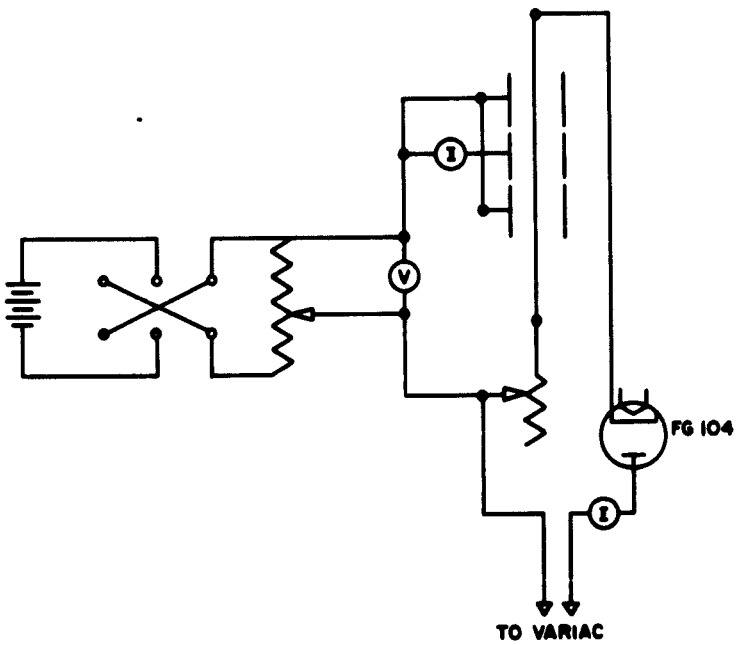

Figure 1 - Circuit Used with Guard Ring Diode

Preliminary measurements were made using a tube which contained a 0.005-inch molybdenum filament to determine the work function of the emitter. After obtaining the correct value for the work function of molybdenum, cesium was dispensed into the tube. Since the temperature of the tube walls determines the cesium vapor pressure, the vapor pressure of cesium was presumed to be 10^{-7} Torr at room temperature. In order to conveniently follow the electron emission, especially in the region between complete coverage of the emitter to complete removal of cesium from molybdenum, the vapor pressure of cesium should be of the order of 10^{-2} Torr. Therefore, to achieve this vapor pressure, the tube was operated at an ambient temperature of 423°K by wrapping heating tapes around the tube. The temperature was monitored with a thermocouple. Also, it was necessary to shield the tube from visible light so that photo currents would be minimized.

In observing the emission from cesium-on-molybdenum, the filament was heated initially to a temperature around 600°K. As the temperature was increased, the emission went through a maximum and then decreased as cesium was removed from the filament. The ambient temperature of the bulb was maintained at 423°K as emission was followed as a function of cathode temperature. The data obtained is shown in Figure 2, Curve A. Although the curve has a maximum in emission at about 830°K, at higher temperatures it does not seem to be very rapidly approaching the Richardson curve for molybdenum.

It can be shown by kinetic theory that a change in the vapor pressure of cesium alters the arrival rate of cesium to the emitter surface. For example, an increase in vapor pressure increases the arrival rate of cesium to the cathode. This, in turn, permits the cathode to be operated at a higher temperature, since the increased arrival rate offsets the increase in the evaporation rate of the cesium. Consequently, the emission maxima will occur at a higher cathode temperature. Thus, attempting to follow the emission maxima, as the vapor pressure was increased, the bulb temperature was raised to 473°K. This change should increase the vapor pressure by almost an order of magnitude. However, no change was observed in the emission maxima. In fact, the data reproduced Curve A of Figure 2. This is believed to indicate that the cesium vapor was not saturated at 473°K or even at 423°K. Although there is sufficient cesium, it is likely that some cesium has combined both with oxides in the tube and deposits from the getter.

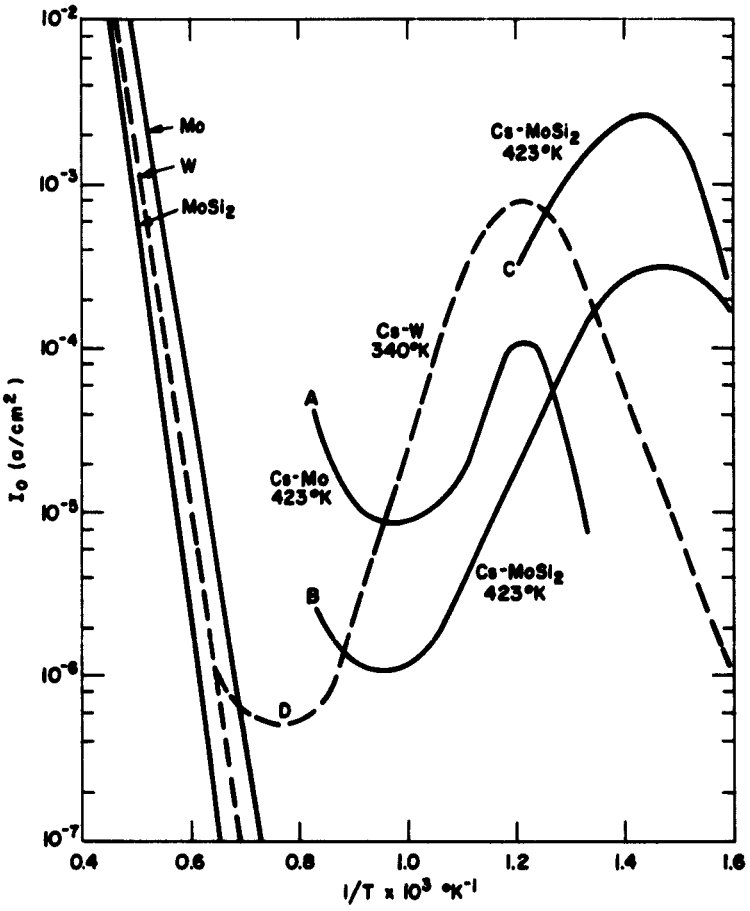

Figure 2 - Field Free Emission as a Function of Temperature for Cesium-on-Refractory Substrates, Preliminary Measurements

It is interesting to note that in the region in which the molybdenum is covered by cesium, the effective work function at 770°K is 1.9 ev as compared to 1.7 ev for cesium-on-tungsten. For comparison purposes, the data reported by Taylor and Langmuir[8] for cesium-on-tungsten at an ambient of 340°K, is plotted as Curve D in Figure 2.

In examining cesium-on-molybdenum, Marchuk[12] found that at an ambient temperature of 473°K and an emitter temperature of 1083°K, the effective work function is 1.7 ev. This data compares favorably with our results even though different experimental techniques were used. Marchuk employed a small loop of molybdenum wire covered with cesium which was mounted between two electrodes. These electrodes were used to produce an intense gas discharge plasma into which the cesium-molybdenum probe was immersed. The arrival of positive ions is used to compensate for the space charge so that electron emission into the plasma is field free.

Following the preliminary examination of the cesium-molybdenum system, a tube containing a molybdenum filament coated with an 0.0008-inch layer of molybdenum silicde was constructed. Cesium was dispensed into the tube as described above. At an ambient temperature of 423°K the emission data plotted in Figure 2, Curve B was obtained. The curve was checked several times and although initially it was reproducible, the emission had dropped by an order of magnitude within 30 hours. On the assumption that some of the available cesium had been "cleaned up," additional cesium was dispensed into the tube. The emission then followed Figure 2, Curve C, giving a work function of 1.4 ev at 630°K for cesium-on-molybdenum silicide.

The ambient temperature was controlled by replacing the heating tapes with an oven in which the entire tube was enclosed. In this way, it was presumed that the vapor pressure of cesium could be controlled more accurately. However, increasing the ambient temperature to 473°K again produced no change in the position of the emission maxima. As in the case of cesium-on-molybdenum, it appeared that the cesium vapor was not saturated and that the emission maxima would probably occur at a higher cathode temperature.

Because of these results, several modifications were made in the succeeding experimental tubes, including the use of oxide-free seals and an increase in the size of the cesium generator.

The oxide free seals were made by beading molybdenum rod with 7060AO glass in a hydrogen atmosphere. These leads were subsequently beaded with 7052FN glass and sealed into a 7052FN flare.

The quantity of cesium chromate was increased so that approximately 200 mg of cesium metal was dispensed into the tube from an appendage which extended approximately five inches from the end of the bulb and was located opposite the base. This permitted heating of the appendage by a small thermostatically controlled oven while the main portion of the tube, including the leads, was heated to approximately 300°C by a second oven.

Using the Schottky method to determine the zero field emission at various temperatures, the work function for molybdenum was found to be 4.2 ev which agrees with published data.

Cesium was then dispensed into the tube and the emission data shown in Figure 3 was obtained. In this illustration, Curves A, B, and C are given for various pressures of cesium produced by ambient temperatures of 293°K, 360°K, and 398°K respectively. Although these curves are not complete, there is a more favorable comparison between the cesium-molybdenum system and the cesium-tungsten system than was noted previously. For example, the emission maxima occurs at a higher cathode temperature as the vapor pressure of cesium increases.

The effective work function of the cesiated molybdenum filament was found to be 1.52 ev at 820°K. This value agrees better with the value obtained by Marchuk[12] than was reported in Scientific Report No. 4 under Contract No. AF19(604)-4093. (See Table I)

Table I - Thermionic Constants for Cesium on Tungsten and Molybdenum

System	ϕ (ev)	A ($a/cm^2/deg^2$)	α ($ev/^oK$)	ϕ (at 820°K)
W-Cs [13]	1.36	3.2	3.2×10^{-4}	1.62
Mo-Cs [12]	1.1	0.123	5.9×10^{-4}	1.58
Mo-Cs (Tube No. 7)	-	-	-	1.52

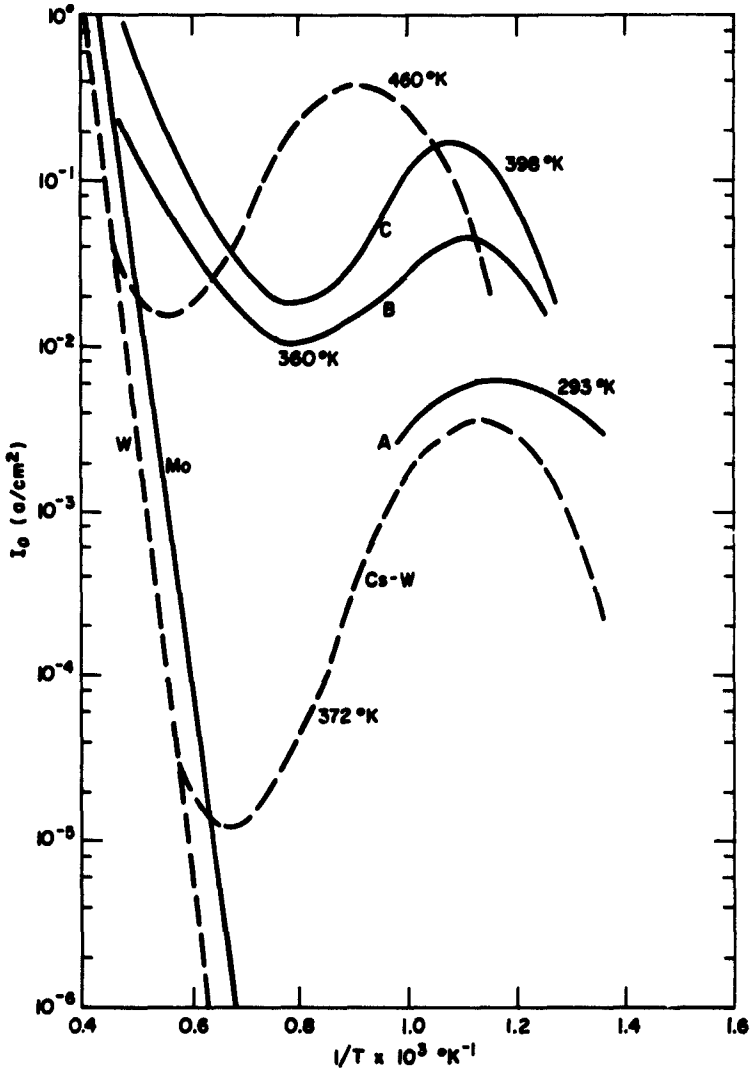

Figure 3 - Field Free Emission as a Function of Temperature for Cesium-on-Refractory Substrates, Later Measurements

Comparison of the data obtained from cesium-on-molybdenum (Figure 3) and the Langmuir data for cesium-tungsten system shows that:

a. For the ambient temperature studied, the emission level appears to be considerably higher for cesium-on-molybdenum than cesium-on-tungsten at the same filament temperature.

b. The change in emission per degree change in ambient temperature for cesium-molybdenum system is much less than Langmuir observed.

While these results might be "explained" in terms of the Langmuir theory, it is more likely that the discrepancies occur in the experimental procedures. Hence, experiments were conducted using the cesium-tungsten system to check the experimental technique by comparing the data with the Langmuir-Taylor[8] results.

Data obtained from the cesium-tungsten system is shown in Figure 4. Although the data yields an S-type curve, these curves do not agree with the Langmuir data[8] (which is given by the dashed lines). Again, two points should be noted. First, there is a slight shift of the experimental data to the right which implies that the filament temperature is generally higher and the measurement is probably in error. Secondly, the vertical displacement of the curves for differing cesium vapor pressures is considerably smaller than expected.

For example, Langmuir's data[8] shows I_{max} for a cesium vapor pressure of $\sim 10^{-6}$ Torr is about three orders of magnitude greater than that for a vapor pressure of $\sim 10^{-4}$ Torr. In this experiment, there is a difference of only one and one-half orders of magnitude. It had been assumed that the coolest portion of the tube envelope determined the vapor pressure. This result suggested that the precise value of the vapor pressure should be determined.

Langmuir and Kingdon[13] found that, if the filament temperature is above 1200°K so that its surface has the work function of clean tungsten and if the collector potential is sufficiently negative, every cesium atom striking the filament leaves it again as a positive ion. Therefore, measurement of the saturation ion current, ν_p, from a unit area of the filament gives a measure of μ_a, the number of atoms striking

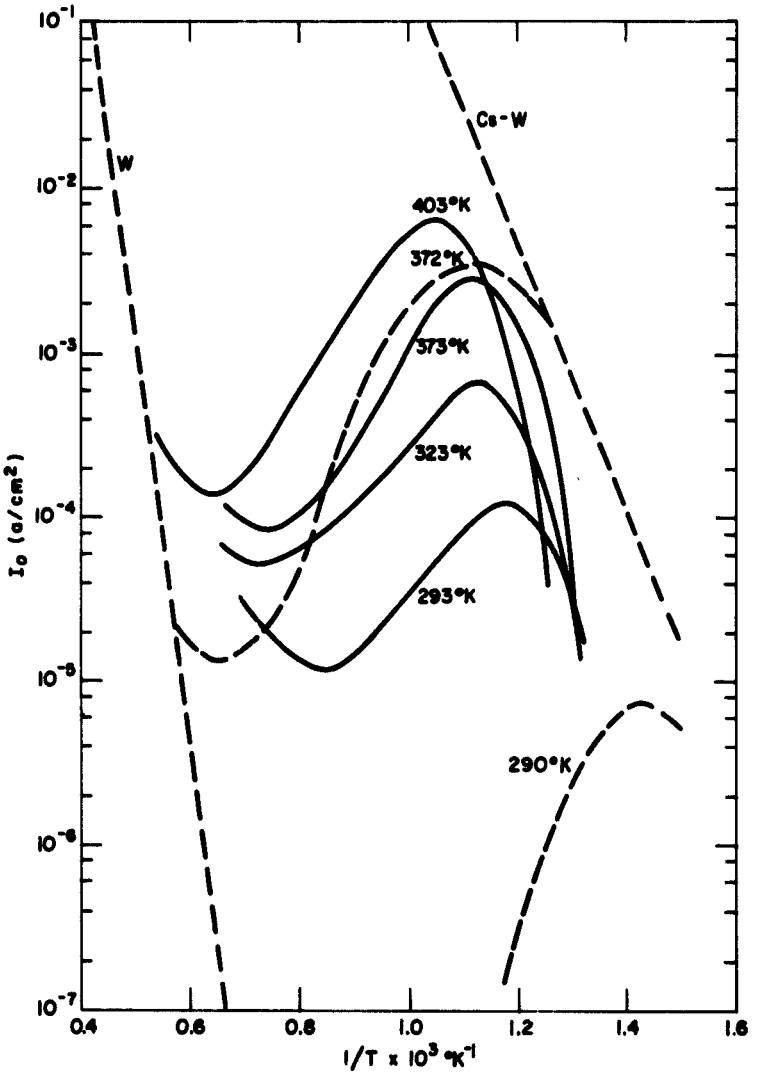

Figure 4 - Field Free Emission as a Function of Temperature for Cesium-on-Tungsten

a unit area of filament per unit time. μ_a is directly proportional to the vapor pressure of the cesium.

In this experiment, it was found that there was virtually no change in the ion current as the bulb temperature was varied over a range of 100°C. This clearly indicated that the vapor pressure of the cesium was not under control.

To improve this situation, it would be necessary to go back to the Langmuir experiment and carefully observe every precaution that was taken. The electrodes must be on the bulb wall; a constant temperature bath must be provided to insure uniform bulb temperature. Also, the tungsten filament should be aged to give a uniform evaporation rate. In addition, it should be pointed out that in the Langmuir experiment, μ_a was varied from 10^{11} to 10^{14} atoms cm^{-2} sec^{-1}, which corresponds to temperatures from 90°K to 290°K. The only data that Langmuir experimentally determined on the cesium-tungsten system was measured in this temperature range. The curves at higher vapor pressure are extrapolations of this data which has not been verified due to the difficulty of the experiment. However, it should be noted that even though it was impossible with the present tubes to determine the surface coverage and arrival rates, μ_a, necessary for theoretical correlations, it was possible to determine the work function of the substrate covered with cesium.

Although the work function value is of interest, more information is needed before a theory can be evolved which would aid in the design of practical cathodes.

C. CONCLUSIONS

A theory has been examined to obtain a relation between electron emission and activator evaporation rate. Such a relation could provide great economy in experimental operations if it could be established by simple experimental means that the system under consideration obeyed the surface equations of state. More specifically, if a system with a substrate characterized by a work function at zero activator surface coverage is activated by a vapor (characterized by an ionization potential) arriving at this surface (that is, by external dispensing), then, with a theory in hand, the electron emission could be computed as a function of cathode temperature for various surface coverages and vapor arrival rates to the surface. Although a relation between the relative evaporation rate of electrons (emission) at zero field and the adatom evaporation

of an ionic film on a metal has been obtained, attempts to obtain experimental data in compliance with the basic assumptions have been unsuccessful. Part of the difficulty was in the experiment itself. For example, the following factors gave particular trouble and even prevented the reproduction of the Langmuir results for cesium-on-tungsten:

(1) It was not possible to maintain a constant and known vapor pressure of cesium during the measurement of the emission for a given cathode temperature.

(2) After changing the ambient temperature, there was little change in vapor pressure of cesium.

(3) Frequently, electrical discharges in the cesium vapor caused erroneous results.

It has been impossible to obtain the data required to support and amend the theory to sufficient accuracy by the simple experimental techniques that would have to be employed if a variety of systems are to be studied. Also, the theory itself would require much more generalization before it would be useful in predicting the properties of even simpler systems under conditions that appear to be of most interest today, such as found in vapor-filled thermionic converters.

Therefore, further attempts in this investigation to study the effect of cesium on various substrates were discontinued in favor of a purely empirical approach, using barium as the internally dispensed activator in combination with various refractory compounds.

SECTION III
PHASE II - INTERNAL DISPENSING

A. GENERAL CONSIDERATIONS

One of the objectives of this program, as mentioned in the INTRODUCTION, was to examine the thermionic properties and evaporation rates of a number of refractory materials with an activating element. The primary purpose of this phase of the study was to determine what effect a refractory substrate might have on the properties of dispenser cathodes activated with barium.

The term "dispenser" has been applied to many different emitters. In fact, Nergaard[14] has suggested that every cathode is a dispenser cathode, while Stout[15] has defined, in a general way, a dispenser cathode as a system that gains its electron emissive power by virtue of material dispensed to its surface. This definition covers a number of systems. As already discussed in SECTION II, the cesium-on-tungsten system is a form of a dispenser cathode in which the activator is dispensed to the surface from an external source, the vapor phase. Most dispenser cathodes that are used in electron devices acquire the emissive material from an internal source. This material may be dispensed to the surface by a number of different mechanisms, such as Knudsen flow, bulk diffusion, grain boundary diffusion, and surface diffusion. It is important to appreciate the complexity of these processes in order to understand the factors influencing the emission mechanism of the dispenser cathode.

The thermionic properties of this type of emitter are usually accounted for on the basis of the monolayer model, which requires the addition of an electro-positive element to a refractory substrate, resulting in the formation of a dipole layer and the lowering of the potential barrier by an amount, $\Delta\phi$. The exact value of $\Delta\phi$ is difficult to predict theoretically and is usually determined by empirical means. Examples of this phenomena have been cited in SECTION I.

It has also been observed[16] that a monolayer of an alkali vapor on a high work-function surface results in a greater lowering of the work

function than when the vapor is deposited on a lower work-function surface.

It is clear that the emission is affected rather markedly when an activator is present in the form of a monolayer or thin film on a refractory substrate. It also raises the question of what effect the substrate-activator combination has on the work function and evaporation rates of thin-film emitters.

In an effort to shed some light on this subject, the thermionic properties of a number of dispenser cathodes composed of a barium dispensing compound in a refractory matrix were examined during the course of this investigation. The experimental techniques and results are discussed in the following paragraphs.

B. EXPERIMENTAL PROCEDURES

The dispenser cathodes examined were prepared by combining a barium dispensing compound with a refractory material such as tungsten, tantalum, or molybdenum or one of the carbides, borides, or silicides of these same elements. In reviewing the literature,[17] a number of general remarks can be made concerning the refractory compounds that are used as the matrix element. The carbides have the highest melting points and probably the greatest stability. The borides, nitrides, and silicides follow in order of decreasing melting point and stability. The latter two generally decompose on melting and very often have relatively high decomposition pressures at temperatures considerably below melting. This was experienced in the case of molybdenum silicide.

Some features of the electron emission are known.[11] The carbides and borides which have been studied, all have work functions which are either approximately equal to or lower than those of the parent metal work functions. The A constant from the Richardson equation varies widely from a small value (0.1 $a/cm^2/deg^2$ or lower) to as high as 5×10^4 $a/cm^2/deg^2$. The high values may merely be due to the improper interpretation of the thermionic data and/or non-equilibrium conditions at the emitter surface. The nitrides have work functions equal to or higher than those of the parent metal but frequently decompose when current is passed through them which is an undesirable property for this study.

1. Matrix Materials

A number of refractory compounds used in this investigation were prepared by A. J. Kiesler of the General Electric Research

Laboratory. The melts were analyzed by x-ray diffraction to accurately identify the structure of the compounds. The results are tabulated in APPENDIX III where a comparison of available, published lattice constants is given with the calculated values of these compounds.

Of the compounds examined, only two specimens, TiB_2 and $MoSi_2$, were found to be relatively pure substances. Most of the other compounds are mixtures containing the intended compound. In many cases, several very weak additional lines appeared which could not be identified. Silicon is present as an impurity in four compounds, two of which, VSi_2 and $BaSi_4$, contain a high abundance of this element. The latter compound cannot actually be identified as $BaSi_4$ since x-ray data is not available in this region of the Ba-Si system. The formula for the WB_2 compound was first reported in the literature, but more recent findings indicate this to be W_2B_5.

2. Cathode Fabrication

Generally, cathodes were made using a refractory compound thoroughly mixed with ten percent by weight of a barium dispensing compound, such as barium silicide or barium aluminide. All of the powders were screened through a 325-mesh sieve. Molybdenum cylinders, 0.438-inch long, 0.125-inch in diameter, and with a wall thickness of 0.005 inch were placed in a suitable die, and a small quantity of the mixed powders was pressed in the cylinder at 70 tons/in^2 to form a planar cathode 0.125 inch in diameter. Then, the cathodes were mounted in test diodes for further processing.

3. Exhaust Station

An exhaust station was constructed to process the experimental tubes under high vacuum conditions. This system included a mechanical pump (Welch Duo-Seal) in series with an oil diffusion pump (Veeco No. EP2AB). A special trap was mounted above the bench. This trap was designed originally as a cold trap, but after a few tests it was demonstrated that sorbents such as activated alumina and zeolite (Linde 13X) in the bottom of the trap were more effective in trapping various gases and vapors than liquid nitrogen. A high-temperature valve that can withstand a bake-out temperature of 450°C was located between the trap and manifold. This permitted isolation of the tube and ion gauge from the remainder of the system for static testing of the tube before

seal-off. After bake-out at a temperature of 425°C for one hour, pressures in the low 10^{-9} Torr range were obtained without the use of a refrigerant in the trap.

4. Emission Data

As described earlier in this report, the zero field emission, I_o, was determined by the retarding potential method during this investigation. After obtaining I_o at some temperature, T, these values were substituted in Equation (1) and ϕ was determined, assuming $A_o = 120$ $a/cm^2/deg^2$ and $r = 0$. This gave the effective work function at a particular temperature. After repeating this procedure for several temperatures, a plot of ϕ versus T was made as in Figure 5. The slope of the curve is the temperature dependance of the work function, $d\phi/dT = \alpha$. The Richardson work function, ϕ_o, can be determined and the general expression for the effective work function can be given in the form of Equation (2).

A number of important factors must be considered when making such measurements. For example, it is absolutely necessary that the space charge minimum between the cathode and collector be less than kT, since the average energy of the electrons emitted in the normal direction from the cathode is kT and any barrier greater than this amount will prevent the measurement of the true emission from the cathode. If the latter condition exists, then, as pointed out by Nottingham,[18] emitters having different emission capabilities appear to be indistinguishable from each other.

An important feature of the retarding potential method is that a plot of the logarithm of the retarding current versus the retarding voltage results in a curve whose slope is e/kT. Since e and k are known, the cathode temperature may be determined. Again, however, the space charge minimum must be less than kT. Also zero field conditions must exist at the collector. The current for this condition can be calculated from an equation given by Nottingham:

$$I_m = 7.7 \times 10^{-12} \, T^{3/2}/W^2 \qquad (8)$$

where W is the anode-cathode spacing and I_m is the maximum current for zero field at the anode. The retarding potential method has been

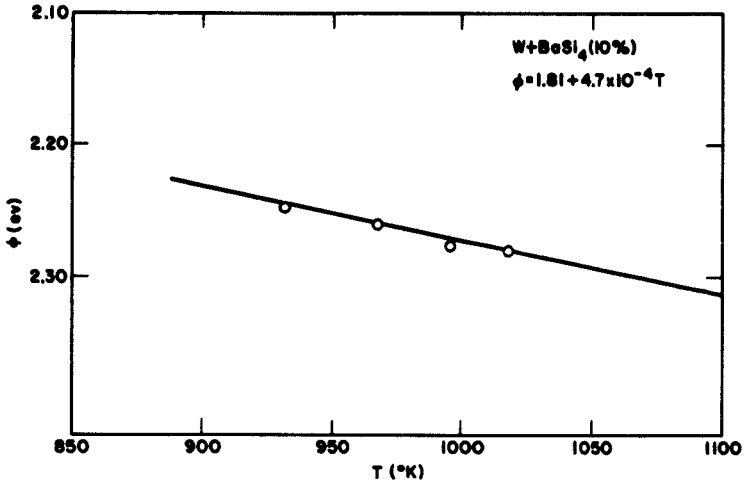

Figure 5 - Work Function versus Temperature

used to evaluate emitter temperatures and properties[19, 20, 21] in various non-parallel structures. However, a magnetic field parallel to the electric field must be used to insure the collection of all electrons with an energy component normal to the emitter surface.

Equipment and circuitry used for measuring zero field emission, I_o, and cathode temperature, T, by the retarding potential method is shown in Figure 6. The salient features were the Leeds and Northrup Type K-2 potentiometer which was used to measure the retarding voltage. This instrument had an extended range permitting voltage measurement ranging from 0.000001 to 16 volts. The micro-microammeter in the collector circuit was a Model 410 Kiethley which has current ranges from 10^{-3} to 10^{-14} amperes. This instrument incorporated a negative feedback circuit so that the voltage drop across the input was constant (0.005 volt). All voltages were derived from storage batteries to prevent erratic fluctuations in voltage. The remainder of the components were standard and used in the conventional manner.

As this program progressed, improvements were made in the retarding potential equipment. The circuit in Figure 6 was modified so that the Type K-2 potentiometer was the voltage source. Also, the batteries were replaced with regulated transistorized power supplies.

Additional improvements and refinements in instrumentation resulted in the construction of a complete and separate unit for measuring the retarding potential characteristic (Figure 7). The two principal components of the equipment were a sensitive micro-microammeter (Kiethley Model 410) and a differential null voltmeter (John Fluke Model 801 D.C.). The equipment shown in Figure 7 was used to determine the thermionic properties of the dispenser cathodes studied in this phase of the investigation.

However, later as the result of the desire to study the effects of environment on the thermionic characteristics of the cathodes, it became evident that a more rapid method of determining the zero field emission and the work function would be necessary.

In processing the test diodes, it had been the practice to display the I versus V characteristic on an X-Y oscilloscope (Tektronix, Inc., Type 536) in order to observe changes in the thermionic properties of the cathode. This was extremely helpful in observing the immediate effects of changes in cathode or anode temperature as well as poisoning

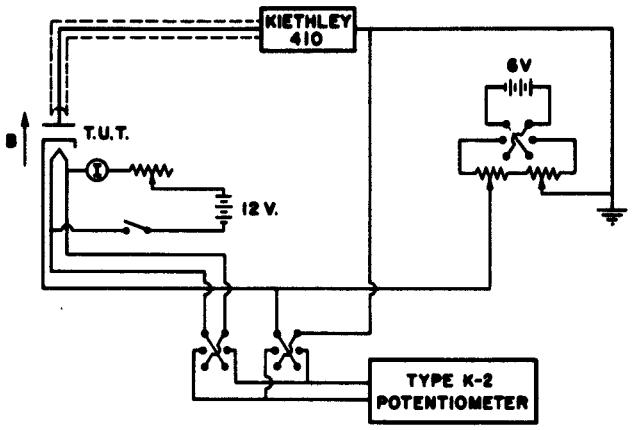

Figure 6 - Retarding Potential Circuit

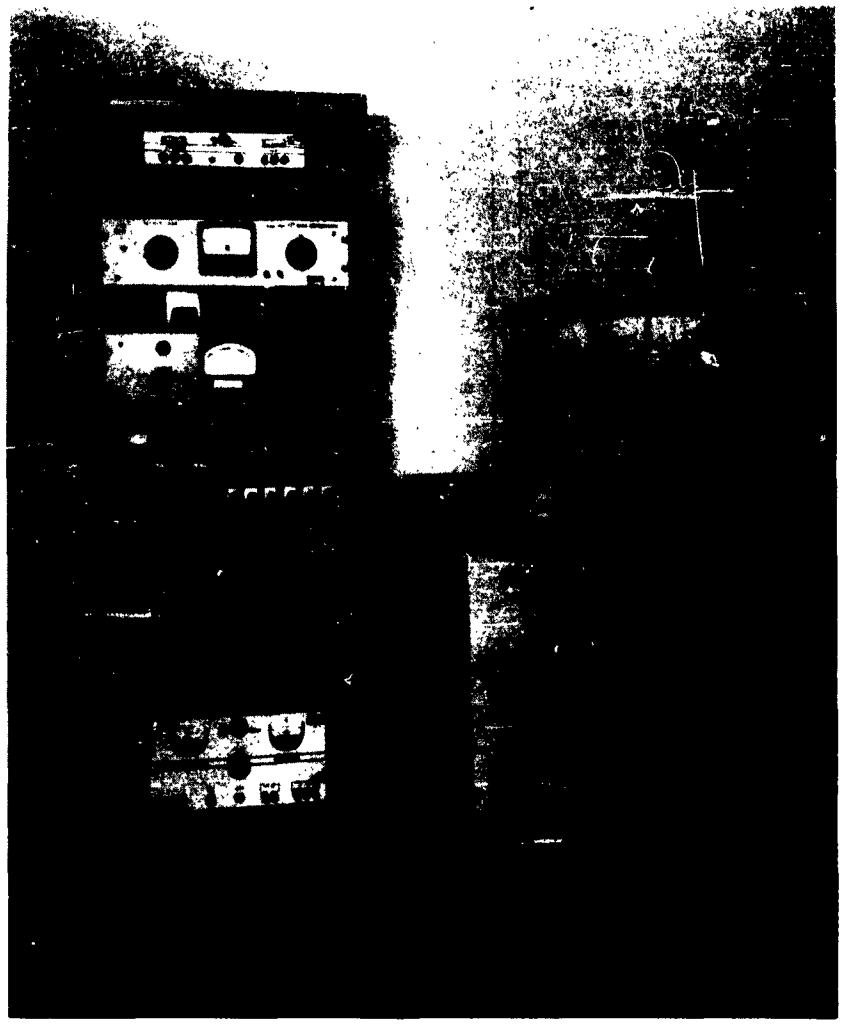

Figure 7 - Equipment Used for Measuring the Retarding Potential Characteristic

phenomena. A typical curve is shown in Figure 8b, along with the circuit used (Figure 8a). Although this type of display was found to be very useful, it did not provide a very convenient means for determining the zero field emission (I_o)

Therefore, the circuit shown in Figure 8a was modified by incorporating a logarithmic amplifier. This was accomplished by removing the y-amplifier plug-in unit (Tektronix, Type G) in the oscilloscope and replacing it with an operational amplifier plug-in unit (Tektronix, Type 0). This unit consisted of three parts: a vertical preamplifier and two operational amplifiers. The vertical preamplifier could be used either as an independent preamplifier as in Figure 8a, or to monitor the output of either operational amplifiers as in Figure 9a.

The operational amplifiers could be used to perform various functions involving integration, differentiation, and amplification by adjusting the input and feedback impedances. Occasionally, it was necessary to add external feedback components to supplement those mounted internally in order to provide a device whose output was proportional to the logarithm of the input. A practical amplifier cannot give a true logarithmic response since the logarithm of zero is infinity and hence could not handle zero input. Also, the logarithm of a negative number is not defined; therefore, a true logarithmic amplifier could not accept a negative input.

An approximate logarithmic output can be achieved with an operational amplifier circuit giving a relation between the input, e_i, and output, e_o, voltages as follows:

$$e_o = 0.98 + (0.40 \log_{10} e_i) \qquad (9)$$

This expression is obtained from the calibration curve shown in Figure 10, and is logarithmic for input voltages between 0.1 and 100 volts. A typical result is shown in Figure 9b. Except for the insertion of the logarithmic amplifier in the circuit, this curve was taken under the same conditions as Figure 8b. With the aid of the calibration curve and the value of the viewing resistor, the y-deflection, which is a logarithmic function of voltage, may be converted to the thermionic emission of the cathode under test.

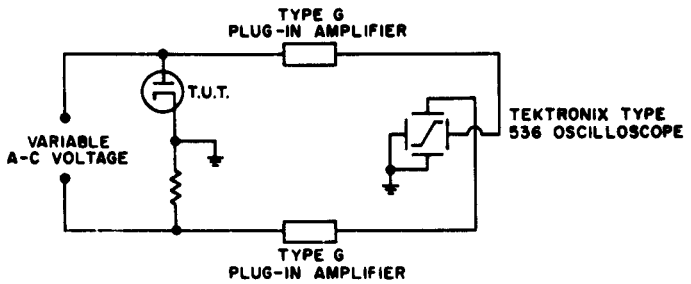

Figure 8a - Circuit for I versus V Characteristic

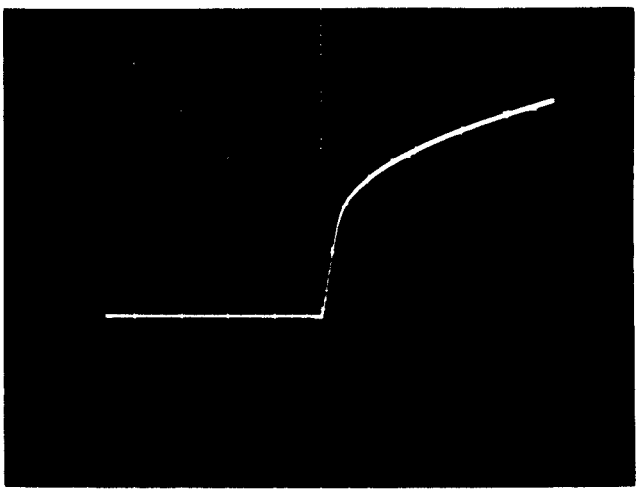

Figure 8b - Typical Trace Obtained Using Circuit in Figure 8a

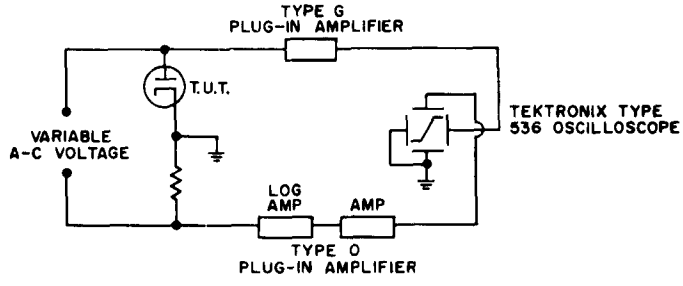

Figure 9a - Circuit for Log I versus V Characteristic

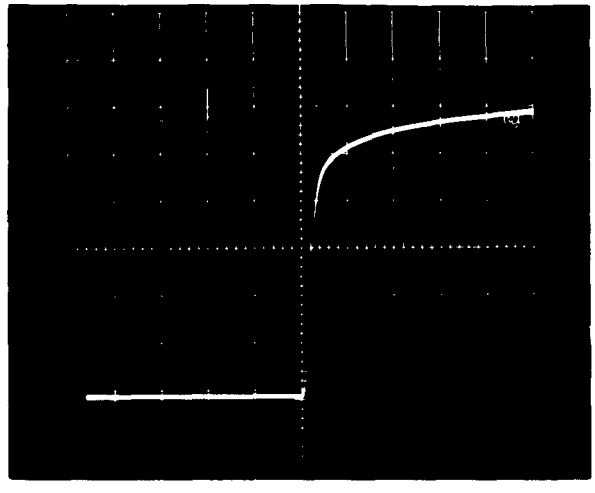

Figure 9b - Typical Trace Obtained Using Circuit in Figure 9a

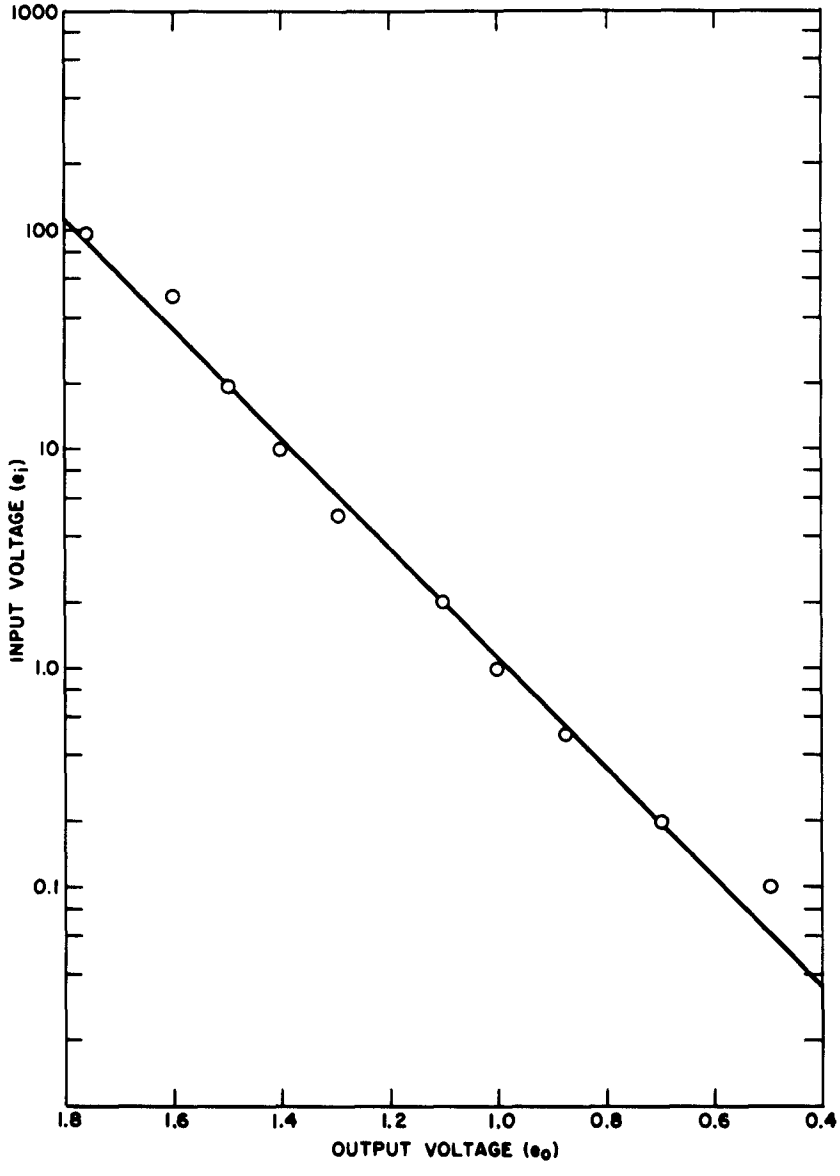

Figure 10 - Output Voltage of Logarithmic Amplifier

Measurements were made on a dispenser cathode (barium orthosilicate in a tungsten matrix) using this method. Typical data, shown in Figure 11, was taken at four different cathode temperatures. The work function determined from this data is:

$$\phi = 1.71 + 4.4 \times 10^{-4} T \quad \text{(ev)} \qquad (10)$$

This data agrees within four percent of that taken by the point-by-point method. Although the technique is limited to certain voltage ranges, it does provide a rapid means for arriving at the cathode work function which should be useful in future studies of the poisoning effect of various gases on the cathode.

5. Evaporation Rates

In the practical application of a cathode, it is necessary to consider not only the work function of the emitter but also the rate at which the activator is evaporated. In general, the evaporation rate determines the life of a dispenser cathode. The excessive loss of the activator also contributes to leakage and grid emission problems. It has been observed qualitatively that the evaporation rate of barium varies considerably, depending upon the composition of the dispenser cathode. The evaporation rate of barium from the systems examined in this investigation was determined by a technique that makes use of x-ray emission spectrography. The principles of this technique are described in APPENDIX IV.

6. Experimental Results

a. Thermionic and Evaporation Rate Data

A number of dispenser type cathode systems were prepared and evaluations made of the thermionic constants and evaporation rates. In general, the procedure was to fabricate a cathode system as described previously, then mount and assemble it into the tube structure. The tube was processed on the vacuum system, described previously, which was capable of pressures of 2×10^{-9} Torr; the seal-off pressure was usually on the low 10^{-8} range. The tube contained a number of anode buttons which were mounted on a track so that they could be manipulated, one at a time, into position over the cathode. The emission data was measured using the first button as the anode. Then, a series of evaporations

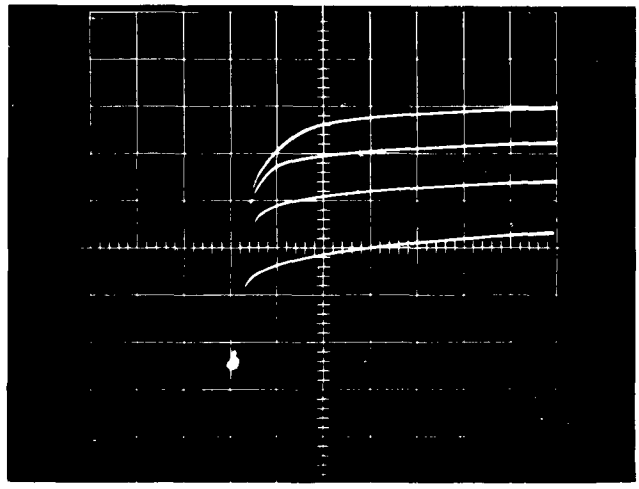

Figure 11 - Log I versus V Characteristics of a Dispenser Cathode at Four Different Temperatures

were made to the remaining buttons at different times and temperatures. The amount of evaporant deposited was analyzed quantitatively by x-ray emission spectrography. The thermionic constants and evaporation rates determined for the cathode systems studied in this investigation are compiled in Table II.

The first column of Table II lists the cathode systems tested. The Richardson work function, ϕ_o, and the temperature coefficient of the work function, α, are given under the heading of thermionic constants. The evaporation rate data can be expressed analytically in the form of the Arrhenius equation:

$$\log W = A - B/T \qquad (11)$$

where W = the evaporation rate in $gm/cm^2/sec$
T = temperature in ^oK
A, B = constants

These values of A and B are tabulated under the evaporation constants.

With the aid of this data, the thermionic and evaporation characteristics of each system are easily determined for any given temperature. An example is given under the heading of Case 1, where the effective work function and evaporation rate are determined for an operating temperature of 1250^oK.

An examination of the data in Table II revealed several points of interest. Initially, a series of cathodes were examined incorporating $BaSi_4$ (10 percent by weight) dispersed in various refractory matrices. The evaporation rates of barium from the various systems including $BaSi_4$ alone were not too different one from another with the exception of tungsten. This implies that the evaporation rate is governed by the thermal dissociation of barium silicide. There is reason to believe that, in the tungsten-barium system silicide,[17] a chemical reaction takes place that reduces the barium silicide at a more rapid rate than thermal reduction of $BaSi_4$ alone, thus increasing the evaporation rate of barium.

Although the evaporation rates in the systems other than tungsten were similar, the thermionic emission properties of these systems had a significant variation. Of the tungsten systems, the tungsten

carbides (WC and W_2C) exhibited the lowest work function while tungsten boride was the highest. The most suitable combination of this series with regard to thermionic emission was WC + $BaSi_4$.

In the tantalum series, tantalum plus barium silicide gave a rather low work function at normal operating temperatures. In fact, it appeared to be one of the best combinations examined thus far. The tantalum-boride system had a rather low evaporation rate, but this was probably the result of inadequate surface coverage as implied by the abnormally high value of α. This particular point will be discussed later.

The molybdenum series exhibited rather high work function and evaporation rates comparable to that of $BaSi_4$.

Barium aluminide ($BaAl_4$) was then substituted for barium silicide in the tungsten series. Results showed that the evaporation rate of barium was much higher than in the system containing barium silicide. Both for barium silicide and barium aluminide, the evaporation rate appeared to be determined principally by the thermal dissociation of the compound.

The next series of cathodes contained alloys composed of barium-strontium silicide, barium-calcium silicide, or barium-strontium-calcium silicide as the dispensing material. It was anticipated and confirmed by experiment that this alloy would reduce the evaporation rate of the barium. The barium-calcium-silicide alloy in particular was very effective when used in tungsten and tungsten-carbide matrices in lowering the evaporation rate of the barium and yet maintaining a low work function.

It is evident from the results obtained in this work that a number of systems exist which can provide a low work-function emitter with favorable emission. The principal difficulty is the excessive evaporation rate of the activator. Therefore, some consideration should be given to the problem of lowering the evaporation rate of the activator.

Basically, the factors that determine the evaporation rate may be divided into two categories: (1) the production of the activating agent, and (2) the transport mechanism by which the activator is dispensed through the matrix and over the emitting surface. In this

Table II - Thermionic and Evaporation Properties of Thermionic Emitters

System*		Thermionic Constants ($\phi = \phi_o + \alpha T$) ϕ_o(ev)	α(ev/°K)	Evaporation Constants log W = A - B/T (W = gm/cm^2/sec) A	B	Case 1 T = 1250° K ϕ(ev)	W(gm/cm^2/sec)
Philips "B"		1.53	5.7×10^{-4}	3.36991	16,989.7	2.24	6×10^{-11}
$BaSi_4$	(100%)	1.59	9.5×10^{-4}	2.6031	12,156.0	2.78	7.5×10^{-8}
W + $BaSi_4$	(10%)	1.81	4.7×10^{-4}	13.3676	21,627.3	2.40	1.16×10^{-4}
		1.88	4.1×10^{-4}	10.0228	17,323.9	2.39	1.45×10^{-4}
WC + $BaSi_4$	(10%)	1.71	4.6×10^{-4}	3.6611	12,730.0	2.28	3.0×10^{-7}
W_2C + $BaSi_4$	(10%)	2.00	2.24×10^{-4}	4.8002	13,357.9	2.28	1.3×10^{-6}
WSi_2 + $BaSi_4$	(10%)	2.25	1.1×10^{-4}	3.2453	13,010.3	2.39	6.8×10^{-8}
W_2B_5 + $BaSi_4$	(10%)	1.12	1.5×10^{-3}	1.4257	12,253.1	3.00	4.2×10^{-9}
Ta + $BaSi_4$	(10%)	1.93	1×10^{-4}	4.9862	12,571.3	2.05	8.5×10^{-6}
$TaSi_2$ + $BaSi_4$	(10%)	1.92	4×10^{-4}	3.3975	12,167.1	2.42	4.6×10^{-7}
TaB_2 + $BaSi_4$	(10%)	1.11	1.2×10^{-3}	-0.5371	8,538.7	2.61	4.2×10^{-8}
Mo_2C + $BaSi_4$	(10%)	1.76	7.8×10^{-4}	2.4119	11,312.8	2.73	2.3×10^{-8}
W_2B_5 + $BaSi_4$	(10%)	2.30	4.3×10^{-4}	7.4565	18,239.1	2.84	6×10^{-8}
TaB_2 + $BaSi_4$	(10%)	1.88	3.9×10^{-4}	5.2961	14,881.2	2.37	2.2×10^{-7}
$MoSi_2$ + $BaSi_4$	(10%)	2.22	3.1×10^{-4}	4.6146	14,313.6	2.61	1.5×10^{-7}
TaC + $BaSi_4$	(10%)	1.79	3.5×10^{-4}	5.7417	15,440.7	2.23	2.6×10^{-7}
Mo_2B + $BaSi_4$	(10%)	2.69	6.2×10^{-4}	Not complete		3.44	-
$BaAl_4$		1.72	6×10^{-4}	3.6493	10,746.3	2.47	9×10^{-6}
W + $BaAl_4$	(10%)	2.30	1.6×10^{-4}	9.7397	19,115.8	2.50	3×10^{-6}
WC + $BaAl_4$	(10%)	2.27	2×10^{-4}	4.0048	14,447.1	2.52	2.8×10^{-8}
W_2C + $BaAl_4$	(10%)	1.91	6×10^{-4}	5.0467	13,631.8	2.66	1.4×10^{-6}
W_2B_5 + $BaAl_4$	(10%)	2.00	6×10^{-4}	4.2080	15,039.9	2.75	1.5×10^{-8}
WSi_2 + $BaAl_4$	(10%)	2.16	1.7×10^{-4}	5.9698	15,326.4	2.37	5.5×10^{-7}
W + ZrH_2 + Ba_2CaWO_6	(0.5%) (9.5%)	1.70	5.9×10^{-4}	0.1466	10,669.5	2.43	4×10^{-9}
$SrSi_4$		1.68	6×10^{-4}	2.7977	11,870.9	2.43	2×10^{-7}

$WC + BaAl_4$	(10%)	2.27	2×10^{-4}	4.0048	14,447.1	2.52	2.8×10^{-8}
$W_2C + BaAl_4$	(10%)	1.91	6×10^{-4}	5.0467	13,631.8	2.66	1.4×10^{-6}
$W_2B_5 + BaAl_4$	(10%)	2.00	6×10^{-4}	4.2080	15,039.9	2.75	1.5×10^{-8}
$WSi_2 + BaAl_4$	(10%)	2.16	1.7×10^{-4}	5.9698	15,326 4	2.37	5.5×10^{-7}
$W + ZrH_2$ + Ba_2CaWO_6	(0.5%) (9.5%)	1.70	5.9×10^{-4}	0.1466	10,669.5	2.43	4×10^{-9}
$SrSi_4$		1.68	6×10^{-4}	2.7977	11,870.9	2.43	2×10^{-7}
$(BaCa)Si_4$		1.84	2×10^{-4}	3.4706	13,521.8	2.09	4×10^{-8}
$(BaSr)Si_4$		1.39	5×10^{-4}	4.3108	14,259.7	2.02	8×10^{-8}
$(BaSrCa)Si_4$		1.76	4×10^{-4}	-	-	2.26	-
$W + (BaCa)Si_4$	(10%)	1.74	4×10^{-4}	10.2339	25,413.6	2.24	8×10^{-11}
$WC + (BaCa)Si_4$	(10%)	1.80	2×10^{-4}	5.2085	16,368.2	2.05	1.3×10^{-8}
$W_2C + (BaCa)Si_4$	(10%)	2.03	2×10^{-4}	11.4337	24,149.7	2.28	1.3×10^{-8}
$W + (BaCa)Si_4$	(10%)	2.00 2.02	3×10^{-4} 5×10^{-4}	0.4967	11,870.9	2.38 2.64	1×10^{-9}
$TaC + (BaCa)Si_4$	(10%)	2.01	3.5×10^{-4}	2.0386	12,009.1	2.45	2.6×10^{-8}
$Ta + (BaCa)Si_4$	(10%)	1.26	7.7×10^{-4}	-	-	2.32	-
$W + Ba_2SiO_4$ + Al	(9.5%) (0.5%)	1.81	3.2×10^{-4}	4.9831	16,726.4	2.21	4×10^{-9}
$Ta + Ba_2SiO_4$ + Al	(9.5%) (0.5%)	1.94	7.3×10^{-4}	-	-	2.85	-
Ba_2SiO_4		2.58	2.4×10^{-4}	-	-	2.88	-
$W + Ba_2TiO_4$ + Al	(9.5%) (0.5%)	1.78	3.4×10^{-4}	-	-	2.20	-
Ba_2TiO_4		1.10	1.3×10^{-3}	-	-	2.73	-
$Ta + Ba_2TiO_4$ + Al	(9.5%) (0.5%)	2.15	5.8×10^{-5}	-	-	2.22	-
$WC + (BaSr)Si_4$	(10%)	1.69	4.65×10^{-4}	2.7630	11,983.7	2.27	1.6×10^{-7}
$W_2C + (BaSr)Si_4$	(10%)	1.49	6.6×10^{-4}	2.7630	11,983.7	2.32	1.6×10^{-7}
$W_2B_5 + (BaSr)Si_4$	(10%)	1.31	1.35×10^{-3}	1.4705	13,251.6	3.00	7.5×10^{-10}
$W + Ba_2 TiO_4$	(10%)	1.92	1.3×10^{-4}	0.5843	13,010.3	2.08	1.5×10^{-10}
$W + Ba_2 SiO_4$ + ZrH_2	(9%) (1%)	2.13	2.5×10^{-4}	1.6507	12,340.8	2.44	3.5×10^{-10}
$Ta + Ba_2 SiO_4$ + Al	(9%) (1%)	3.36	1.3×10^{-4}	7.5833	25,006.0	3.52	3.8×10^{-13}

W + $(BaCa)Si_4$	(10%)	1.74	4×10^{-4}	10.2339	25,413.6	2.24	8×10^{-11}
WC + $(BaCa)Si_4$	(10%)	1.80	2×10^{-4}	5.2085	16,368.2	2.05	1.3×10^{-8}
W_2C + $(BaCa)Si_4$	(10%)	2.03	2×10^{-4}	11.4337	24,149.7	2.28	1.3×10^{-8}
W + $(BaCa)Si_4$	(10%)	2.00 2.02	3×10^{-4} 5×10^{-4}	0.4967	11,870.9	2.38 2.64	1×10^{-9}
TaC + $(BaCa)Si_4$	(10%)	2.01	3.5×10^{-4}	2.0386	12,009.1	2.45	2.6×10^{-8}
Ta + $(BaCa)Si_4$	(10%)	1.26	7.7×10^{-4}	-	-	2.32	-
W + Ba_2SiO_4 + Al	(9.5%) (0.5%)	1.81	3.2×10^{-4}	4.9831	16,726.4	2.21	4×10^{-9}
Ta + Ba_2SiO_4 + Al	(9.5%) (0.5%)	1.94	7.3×10^{-4}	-	-	2.85	-
Ba_2SiO_4		2.58	2.4×10^{-4}	-	-	2.88	-
W + Ba_2TiO_4 + Al	(9.5%) (0.5%)	1.78	3.4×10^{-4}	-	-	2.20	-
Ba_2TiO_4		1.10	1.3×10^{-3}	-	-	2.73	-
Ta + Ba_2TiO_4 + Al	(9.5%) (0.5%)	2.15	5.8×10^{-5}	-	-	2.22	-
WC + $(BaSr)Si_4$	(10%)	1.69	4.65×10^{-4}	2.7630	11,983.7	2.27	1.6×10^{-7}
W_2C + $(BaSr)Si_4$	(10%)	1.49	6.6×10^{-4}	2.7630	11,983.7	2.32	1.6×10^{-7}
W_2B_5 + $(BaSr)Si_4$	(10%)	1.31	1.35×10^{-3}	1.4705	13,251.6	3.00	7.5×10^{-10}
W + Ba_2TiO_4	(10%)	1.92	1.3×10^{-4}	0.5843	13,010.3	2.08	1.5×10^{-10}
W + Ba_2SiO_4 + ZrH_2	(9%) (1%)	2.13	2.5×10^{-4}	1.6507	12,340.8	2.44	3.5×10^{-10}
Ta + Ba_2SiO_4 + Al	(9%) (1%)	3.36	1.3×10^{-4}	7.5833	25,006.0	3.52	3.8×10^{-13}
Ta + $(Ba_2Ca)WO_6$	(10%)	3.10	1.0×10^{-4}	6.1848	22,552.7	3.22	1.4×10^{-14}
W + Ba_2SiO_4 + ZH_2 + $CaCO_3$	(10%) (1%) (1%)	1.85	2.2×10^{-4}	3.6134	17,727.6	2.12	2.7×10^{-11}
W + $BaSi_4$ + Pt	(10%)	2.09	1.1×10^{-4}	2.6405	14,011.5	2.23	2.7×10^{-9}
W + Ba_2TiO_4 + $CaCO_3$ + tungsten layer	(10%) (1%)	1.83	2.5×10^{-4}	0.5483	13,348.9	2.14	7.4×10^{-11}

*The percentage denotes composition by weight

investigation, attempts have been made to keep all other factors constant and vary only the production of the activating agent by using different barium dispensing compounds.

By controlling the rate of production of the barium, it is possible to reduce the evaporation rate of barium. An example is the dispenser cathode,[22] which uses barium aluminate as the dispensing compound and depends upon a chemical reaction between tungsten and barium aluminate to generate the barium necessary for activation.

Another dispenser cathode system has been reported[23, 24] recently which uses an alkaline earth tungstate as the barium dispensing material. In this type of system, it is necessary to incorporate a reducing impurity with the tungstate to produce free barium, as shown by Eisenstein, John, and Affleck.[25] Pressed cathodes tested by Huber and Freytag[23] and Mel'nikov et al[24] consisted of 90 percent tungsten, 9.5 percent barium tungstate and 0.5 percent aluminum. Although emission values of 6 to 7 a/cm^2 at 1130°C to 1150°C were obtained, the emission constants and evaporation rates were not reported. In order to evaluate this system, a cathode was prepared consisting of 9.5 percent barium-calcium tungstate (Ba_2CaWO_6) with 0.5 percent zirconium hydride (ZrH_2) and 90 percent tungsten compacted at 70 tons/in^2. Although others[23, 24] had used aluminum as the reducing agent, it was suggested that a more active element such as zirconium be used.* Although the work function of this cathode was similar to the work function of other systems examined, the evaporation rate was somewhat improved.

There is no reason to believe that other systems should not exhibit similar properties. For example, Eisenstein, John, and Affleck[25] also reported that reactions such as the following take place:

$$Ba_2SiO_4 + 2Al \rightarrow BaAl_2O_4 + Si + Ba \qquad (12)$$

$$Ba_2TiO_4 + 2Al \rightarrow BaAl_2O_4 + Ti + Ba \qquad (13)$$

In the study of various dispenser cathode systems, it becomes clear that such reactions might very well be useful as a barium

*This innovation was suggested by M. D. Gibbons and I. T. Saldi of the General Electric Research Laboratory.

producing agent. Several systems are reported in Table II which have used Ba_2SiO_4 and Ba_2TiO_4 with a reducing agent such as Aℓ or Zr.

b. Control of the Evaporation Rate

In examining some of the factors influencing the evaporation rate, several ways are available in which one might attempt to lower the rate. For example, if the surface were devoid of emitting pore ends which can evaporate material directly without diffusing through the matrix, the loss of barium-barium oxide should be reduced. Therefore, a cathode was made whose surface consisted of pressed tungsten powder about 0.002-inch thick. A mixture of tungsten (90 percent) plus barium titanate (9 percent) and $CaCO_3$ (1 percent) was pressed into place in back of this tungsten layer. The evaporation rate of barium from $W + Ba_2TiO_4$ was 1.5×10^{-10} gm/cm^2/sec at 1250°K, where, with the tungsten layer in place, the evaporation rate was 7.4×10^{-11} gm/cm^2/sec.

Another method of lowering the evaporation rate is to place a material on the cathode surface over which the barium can readily migrate and yet is bound, so that average life time of a barium atom is long. Recent work by Marchuk[26] shows that the mean life time of a barium atom on a platinum surface is about 60 times greater than for tungsten. This suggested that perhaps a thin layer of platinum evaporated onto the cathode surface might aid in retaining the barium and lowering the evaporation rate. Therefore, platinum was evaporated onto a cathode of tungsten (90 percent) and barium silicide (10 percent). (The tungsten-barium silicide system has been examined before and has an evaporation rate of 1.4×10^{-4} gm/cm^2/sec at 1250°K.) With platinum on the surface, the evaporation rate of barium was lowered to 2.7×10^{-9} gm/cm^2/sec without affecting the thermionic properties.

A third effort resulted in reducing the evaporation by simply adding $CaCO_3$ to the mixture. It is believed that, upon conversion, the CaO fills the pores and provides a structure which impedes the diffusion of barium to the emitter surface and aids in retaining the barium. The use of CaO in a dispenser system has been used[27, 28] successfully before to reduce the evaporation rate of barium.

Still another method to control the evaporation is to control the porosity of the matrix.[5] This technique is well known and will not be discussed here.

Since some of the systems recently examined exhibited thermionic constants and evaporation rates that are very satisfactory for use as high-current density emitters, tests were initiated to determine the life characteristics. Two cathodes were fabricated using a system composed of a tungsten matrix containing barium orthosilicate (10 percent by weight), zirconium hydride (1 percent), and calcium carbonate (1 percent). These cathodes were mounted in diodes. After the usual processing and activation, the diodes were put on life test. Both tubes are operating under space charge limited conditions at a temperature of 1075°C. One tube has been on life test for 11,500 hours at 0.5 a/cm^2 d-c, while the second tube has been on life test for 11,000 hours at 1.0 a/cm^2 d-c. At present there is no indication of degradation.

c. Interpretation of the Thermionic Emission Data

During the course of this investigation and the determination of the thermionic constants, ϕ_o and α, it was observed that the temperature coefficient of the work function, α, occasionally had values in the 10^{-3} ev/°K range. A number of intrinsic effects may contribute to the temperature dependence of the work function. These effects have been discussed by Herring and Nichols[29] and, when combined, produce a value for α which is in the range of 10^{-4} ev/°K or less.

Although the temperature dependence of the work function depends on a number of factors, the one having the most profound effect in actual practice is the stability and uniformity of the emitting surface. Taylor and Langmuir[8] have shown the effect on the emission from tungsten as a function of coverage by externally dispensed cesium. If the familiar S-type curve for the W-Cs system is plotted, as in Figure 12, in terms of the effective work function versus temperature, some of the effects of surface coverage on the interpretation of this data may be delineated. For example, if data for only those portions of the curve marked A, B, and C were examined, three completely different values for ϕ and α would be obtained. In region A, the constants would describe a cesium-on-tungsten surface, while region C would represent a clean tungsten surface. Region B would be most confusing if it happened to be the only region examined. Here, a very low value for ϕ_o would be obtained, perhaps even a negative value. Also, the temperature dependent term, strongly affected by the surface coverage, would have a rather high value and hence an extremely low value for the Richardson constant, A, would be realized. Although the properties of

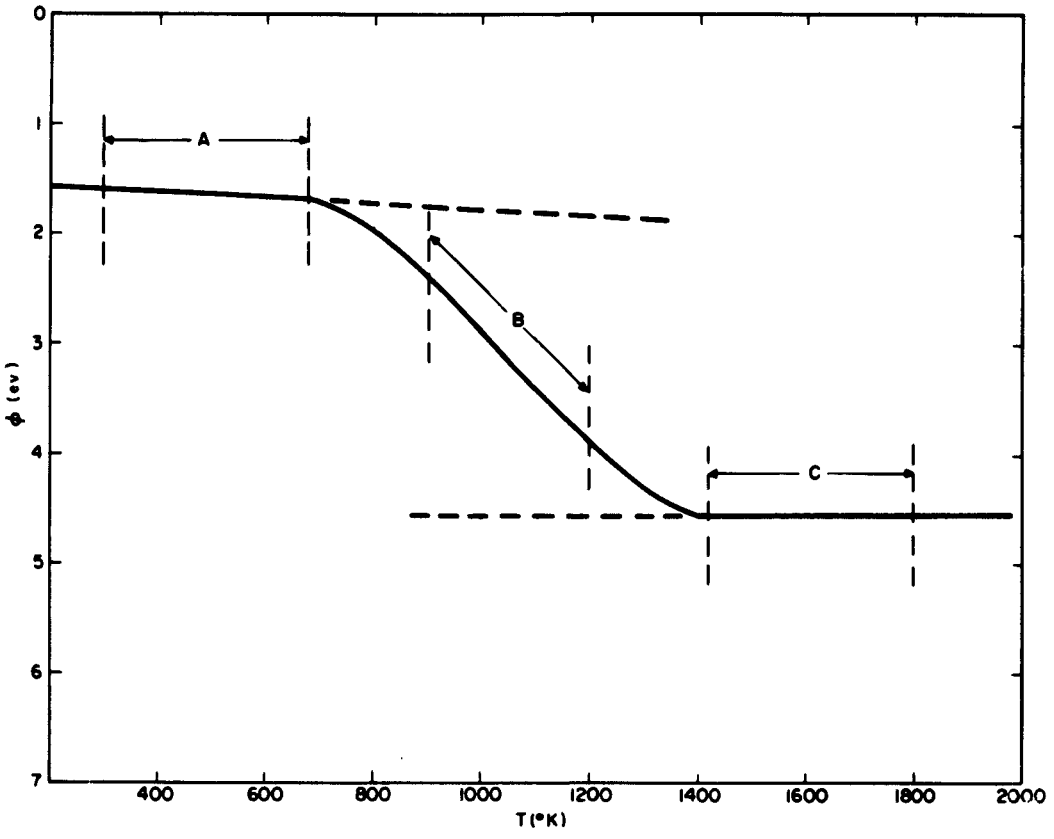

Figure 12 - Cesium-on-Tungsten ($\mu_a = 10^{15}$ atoms/cm^2/sec)
Work Function versus Temperature

each region may be expressed in terms of ϕ_o and α, these constants do not characterize the emission over the entire temperature range. It is very clear that the stability and uniformity of the emitter surface in the temperature range of interest have an important bearing on the emission constants and the effective work function.

A typical example of this phenomena was observed during this investigation in the case of the $MO_2B + BaSi_4$ cathode. In Figure 13, two retarding potential curves are shown for the $Mo_2B + BaSi_4$ system. Curve A was first observed with what appeared to be two breaks in it. After establishing the reproducibility of the curve the cathode was flashed briefly at a temperature of 1500°C. Then, the temperature was lowered and Curve B observed. This is the type of curve normally obtained by the retarding potential method and does not have the second break (at least in the range measured). This effect is attributed to the fact that initially the cathode surface consisted of a relatively large area of high work function and a very small area of low work function. Curve A probably represents the superposition of the retarding potential curves for these two areas. Upon flashing, the activator diffuses over more of the surface and some is evaporated onto the anode. Curve B represents the condition in which the surface is approaching complete coverage. The curve has been displaced to the right as a result of the change in contact potential between anode and cathode.

In subsequent tests the processing schedule was modified to include flashing the cathode at elevated temperatures to insure adequate surface coverage. The temperature coefficient was found to be much lower and yielded a reasonable emission constant.

Another factor that can very subtly influence the temperature dependence of the work function is the manner in which the zero field emission is determined. In this work, the zero field emission, I, is determined from a retarding potential plot (as described in Scientific Report No. 2 of Contract No. AF19(604)-4093; AFCRC-TN-59-104). It is necessary to extend the straight line portions of the retarding curve and the saturation region of the curve to a point of intersection in order to determine I_o. At low cathode temperatures and at low currents, the retarding curve breaks rather sharply and the region of saturated emission is well defined by data points which lie on a straight line. However, at higher temperatures and consequently at higher current densities, the break in the curve is not well defined because of space charge effects. In fact, there is considerable difficulty in determining the straight line

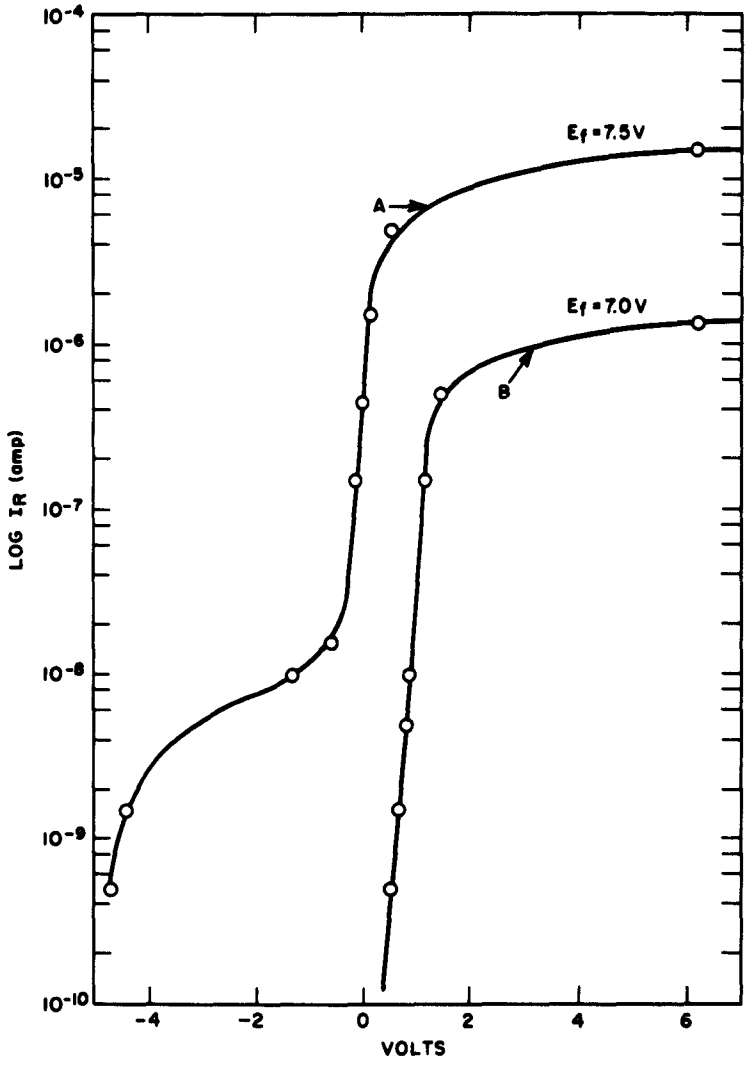

Figure 13 - Retarding Potential Characteristic of $Mo_2B + BaSi_4$

portion of the curve in the saturation region. Obviously, this may result in a considerable error in the determination of I_o and the value of the effective work function. Looking again at Figure 12, a curve similar to the regions A and B may be obtained in a vacuum diode when space charge influences the data. Measurements of I_o without space charge being present result in region A of the curve, while at higher currents the space charge affects the accuracy with which I_o and also ϕ is determined. The space charge, then, limits the current in the tube, and region B is erroneously taken to be the temperature dependence of the work function which again results in an α that is $\sim 10^{-3}$ ev/^{o}K and a ϕ_o that is < 1 ev and is sometimes even negative.

Therefore, in order to determine the temperature variation of the work function in the temperature range in which the cathode normally operates, it is necessary to measure I_o in this same range. To accomplish this in a practical manner presents several problems. First, for a number of cathode systems, the power delivered to the anode at rather nominal voltages can result in anode dissipation problems. Also, the electrode spacing may require rather high voltages to obtain saturated emission.

Secondly, there is the problem of obtaining the zero field emission from some form of the I-V characteristic. (The shortcomings of the intersection method and the retarding potential curve have already been discussed.) This is not an uncommon problem and has been examined by others. In fact, Ferris[30] and Nottingham[18] have independently proposed a method to aid in solving just this problem. An attempt was made in this investigation to use the method worked out by Nottingham, the details of which are discussed in the Handbuch der Physik.[18] Briefly, this technique requires that if the applied voltage in the test diode is such that space charge exists between the emitter and collector, then the variation in current with applied voltage follows a universal curve, as in Figure 14. This curve plots the log I/I_R, which is the ratio of electron emission to the emission when there is zero field at the collector, against the ratio of the true retarding potential to the voltage equivalent of the temperature, V/V_T. The voltage equivalent of temperature is determined from the relation:

$$V_T = \frac{kT}{e} = \frac{T}{11,600} \qquad (14)$$

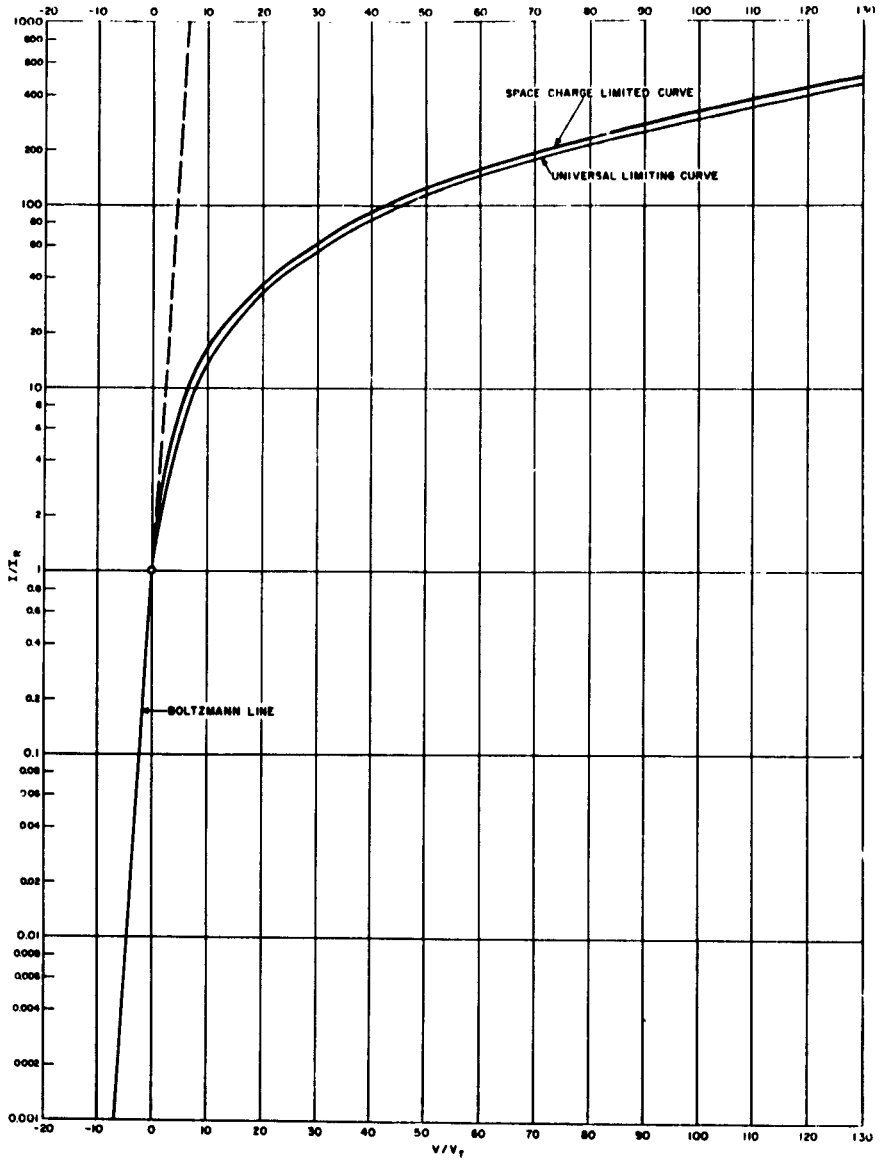

Figure 14 - Master Curves of Diode Characteristics as Proposed by W. B. Nottingham

The lower portion of the curve, below $V/V_T = 0$, is just the Boltzmann line and has a slope of 0.4343. For positive ratios, two curves are shown. The upper one is the space charge limited curve while the lower one is the universal limiting curve.

In practice the log I is plotted versus V_a/V_T (where V_a is the applied voltage) on the same scale as the master curves. By superimposing the experimental curve upon the master curve and by shifting the curves vertically and horizontally with respect to one another, a fit may be obtained along the Boltzmann line and a portion of the space charge limited curve. At some point, the experimental data will break away from the space charge limited curve and cross the universal limiting curve. This point of intersection is the point for which there is zero field at the emitter, and hence I_o is determined.

This technique has been applied to a number of systems. The work function versus temperature for one such system is shown in Figure 15. The data again shows a curve with region having two different slopes. Since care was taken to eliminate space charge effects, the change in slope above a temperature of 800°K is attributed to a change in the surface coverage of the emitter. Attempts to completely remove all barium from the surface and reach the curve for TaC resulted in a heater failure.

d. Environmental Effects

In addition to the thermionic, evaporation, and life characteristics, another important aspect of cathode performance is the environment in which it must operate. During this investigation, plans were to study the effect of various gases (such as O_2, H_2, CO, and CO_2) on the thermionic emission of several dispenser cathodes with the aid of a General Electric Partial Pressure Analyzer. Unfortunately, considerable difficulty was encountered with the Partial Pressure Analyzer when used in conjunction with the exhaust station described earlier. The problem centered around the electron multiplier response of the Partial Pressure Analyzer.

At high system pressures (5×10^{-6} Torr) seen during processing, the mass spectrum peaks tended to increase beyond a value actually representing the partial pressure of that mass. This was more pronounced on large peaks and depended on the dwell time on the peak. Moving off the peak resulted in a slow decay to the base line, often

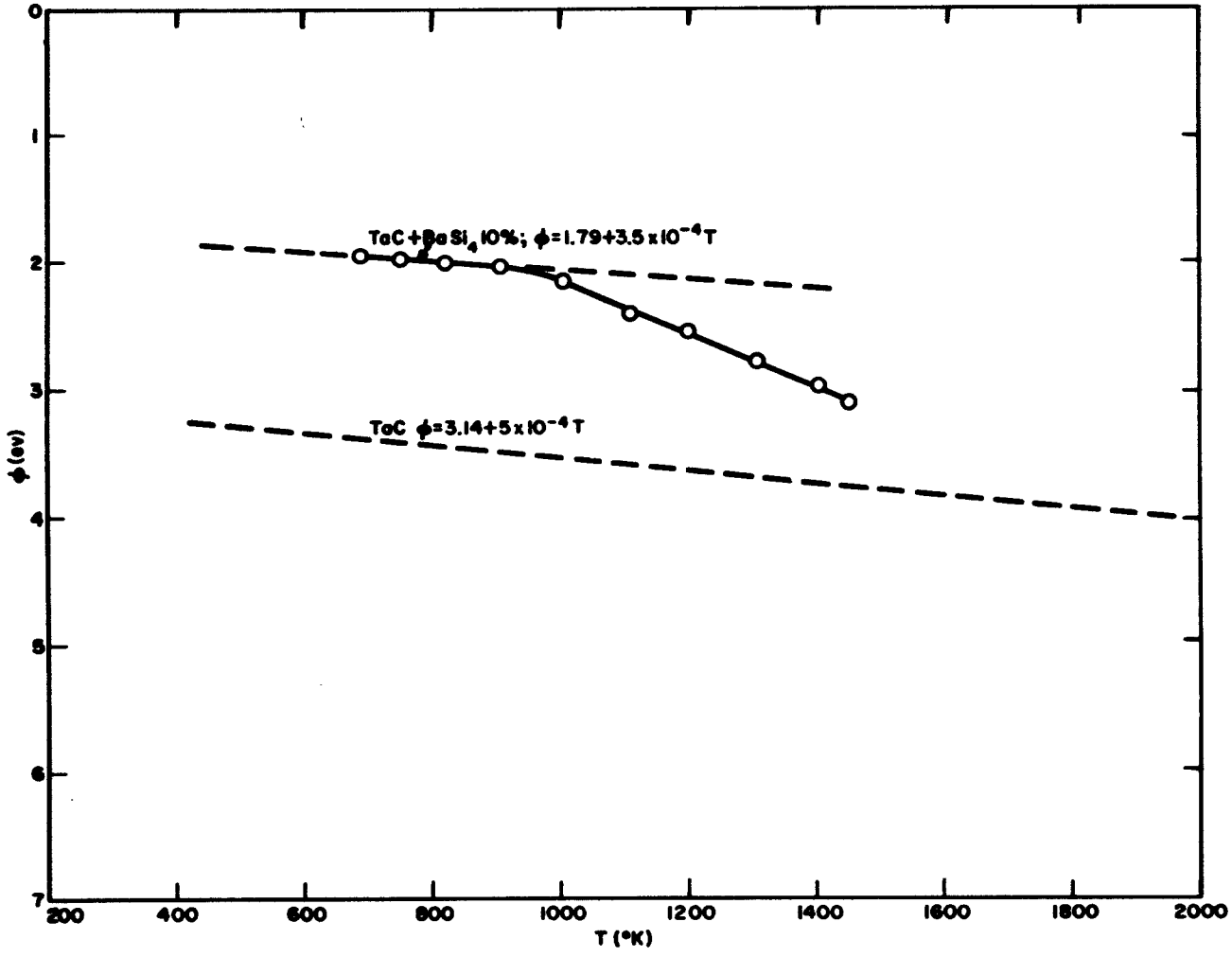

Figure 15 - Work Function versus Temperature

masking small adjacent peaks. After making a number of tests and checking all the systems involved, the phenomena observed may be explained in the following manner.

The electron multiplier contains secondary electron emitter surfaces formed by carefully controlled oxidation of alloys such as silver magnesium. The MgO film which provides the secondary emission must be limited in thickness for stable multiplier operation. One of the techniques for forming these MgO films is to heat the Ag-Mg alloy in water vapor, with pressures of 10^{-4} Torr and temperatures of 550°C being typical. This means that if multipliers are heated on vacuum systems in the presence of large amounts of water vapor, additional MgO will be formed. Malter[31] has established that oxide films, upon electron bombardment, can emit secondary electrons which reach a peak value of emission current some time after the start of bombardment and continue emitting in a decaying fashion after bombardment. If the MgO film has a high resistivity, a positive charge is built up upon electron bombardment, creating fields of such intensity that field emission is caused from the Ag-Mg and MgO. Very thin or patchy films display the field emission to a negligible degree, so no difficulty is encountered as long as the MgO thickness remains small, i.e., no water vapor in the system. An important point is to realize that the source of water vapor in the system was the sorbent in the trap (both activated alumina and zeolite were used). Enough water vapor is evolved from the sorbent during bake-out to raise the vapor pressure in the system to the micron range while the multiplier dynodes are at temperatures of 425°C. Hence, MgO is likely to form and the Malter effect will occur. To eliminate this problem, the trap must be baked to a temperature of 400°C while keeping the multiplier cold. This can be done easily with electrical heating tape.

Unfortunately, no convenient method is available to date for reclaiming multipliers damaged by water vapor and the electron multiplier must be replaced in the Partial Pressure Analyzer before these studies may be continued.

CONCLUSIONS

A number of the systems studied during this phase of the investigation exhibited a rather high-temperature dependence of the work function. These cases were shown to be the result of "patchy" emitting surfaces. Also, some of the systems were difficult to activate at all and

the desired low work function was never obtained. However, 70 percent of all systems examined and reported in this investigation have effective work functions of 2.50 ev or less at 1250°K, and 50 percent of these cathodes have an effective work function of 2.28 ev or less, or an average effective work function $\phi = 2.20$ ev. It should be remembered that these systems have various matrices and various combinations of barium dispensing material and reducing agents (see Table II). Yet quite a high percentage of the systems exhibit similar thermionic properties and compare favorably with other dispenser cathodes, such as the barium-nickel matrix, the L-cathode, and the barium aluminate pressed and impregnated structure (see Table III).

Table III - Effective Work Function of Several Dispenser Cathodes

System	ϕ (ev) $T = 1250°K$
Barium-nickel[1]	1.94
L-cathode[5]	2.09
Barium aluminate (pressed)[32]	2.20
Barium aluminate (impregnated)[22]	2.24

The properties of these systems are discussed in SECTION IV, DISCUSSION OF RESULTS and interpreted in terms of the emission mechanism.

SECTION IV
DISCUSSION OF RESULTS

Since a number of dispenser cathode systems were examined in this investigation and the thermionic constants and evaporation rates reported, it is appropriate at this time to begin examining some aspects of the emission mechanism in these systems and to compare these results with other data with a view toward arriving at a better understanding of dispenser cathode systems in general.

The term "dispenser cathode" was applied to various types of thermionic emitter systems and, as proposed by Stout, [15] may be defined as a "cathode that gains its electron emissive power by virtue of material dispensed to its surface." The emissive material may be dispensed to the cathode surface by external or internal source and ideally would uniformly cover the emitting surface a monolayer thick.

An example of an "external dispenser" is the cesium-on-tungsten system in which cesium is deposited on tungsten from the vapor phase. This method is used in cesium vapor thermionic converters.

However, the most common method is that of internal dispensing. There are many different ways of doing this practically. The important thing is to dispense the emission material to the matrix surface so that a rather uniform layer is formed over the surface, resulting in a lowering of the work function. At least four important factors are involved in this dispensing action and the maintenance of a uniform surface.

1. The production of the emissive material, usually an electro-positive atom.

2. The transport of the emissive material through the matrix to the surface. This may take place by Knudsen flow through the pores, surface migration, bulk diffusion, or grain boundary diffusion.

3. The diffusion of the emissive material over the cathode surface.

4. The evaporation of the emissive material from the cathode surface.

Each of these factors is a rate process which is temperature dependent. The probability that each of these processes has exactly the same rate, at a given temperature, necessary to maintain a monolayer coverage of the emissive material on the cathode surface is highly improbable. If one or more of these processes proceeds at a much greater rate than the others, then the surface coverage, θ, may be either greater or less than unity.

For $\theta > 1$, the surface may have many adsorbed layers and its thermionic properties are not necessarily characteristic of an adsorbed monolayer on a refractory substrate. The surface is more of a composite containing many layers of the adsorbed atom as well as adsorbed gas. For example, in the case of barium there certainly is a mixture of Ba and BaO.

For $\theta < 1$, the emission originates from a "patchy" surface where some areas are composed of the dispensed material, others are partially covered, and in some cases the substrate will not be covered at all. However, in the case of the well activated dispenser cathode, the emission source is most likely a thin film of Ba-BaO.

Since the emitting surface of a barium dispenser cathode is believed to be a thin film of Ba-BaO, it is not surprising that the thermionic properties are similar. Of course, many different materials may be used to obtain the thin film of Ba-BaO (Table II). Therefore, it would seem that there would be little difficulty in making a practical high-current density cathode.

However, one has only to look at the evaporation rates for these same systems (Table II) to find that the primary difficulty is that of maintaining a low evaporation rate of the emissive material. This difficulty may be overcome, for a number of ways exist in which the evaporation rate may be lowered and still maintain the desirable thermionic characteristic. The effect of altering the barium dispensing compound and the addition of $CaCO_3$ on the evaporation rate is shown in Table IV.

Table IV - Effect of Various Barium Sources and Additions on Evaporation Rate

System	Evaporation Rate T = 1250°K (W = gm/cm^2/sec)
W + $BaSi_4$	1.2×10^{-4}
W + $BaAl_4$	3×10^{-6}
W + $(BaCa)Si_4$	8×10^{-11}
W + Ba_2SiO_4 + Al	4×10^{-9}
W + Ba_2SiO_4 + ZrH_2	3.5×10^{-10}
W + Ba_2SiO_4 + ZrH_2 + $CaCO_3$	2.7×10^{-11}

As has been pointed out, several temperature dependent processes are responsible in dispensing barium uniformly over the cathode surface and, except in special cases where there is exactly a monolayer coverage, the effect of various substrates on the work function is negligible. However, it should be noted that the substrate may have a secondary effect on the thermionic properties of a cathode insofar as the substrate may aid or impede the dispensing of the emissive material to the cathode surface.

It is recognized that the emitting surface of a dispenser cathode is very complex. The emission may originate from either a uniform coating many layers thick of barium-barium oxide, isolated active patches, pore ends, or a combination of all of these sources.

In this investigation an attempt has been made to determine the effect of the substrate-activator combination on the work function and evaporation rates of thin-film emitters. If the activator covers the substrate uniformly one monolayer thick, then the work function of the substrate would presumably have a considerable effect on the change in work function resulting from the adsorbed dipole. In fact, data confirming this has been reported[16] for the system of Cs-on-Ta.

Nergaard[14] has suggested that "monolayer emitters do not exist," and that dispenser cathodes can best be described in terms of a semi-conductor model. When the results of the systems listed in Table II are reviewed in terms of the semi-conductor model, it is not surprising that the emission properties of the systems are so similar. The emission of these systems must originate from Ba-BaO films thick enough to exhibit the properties of an N-type semi-conductor and to screen any effect the base metal might have on a dipole layer. Also, the similarity in the evaporation rates of barium from these systems to that of barium from barium oxide coating suggests the presence of a Ba-BaO film.

SECTION V
SUMMARY

In summarizing the results of this investigation, the following rather salient points may be stated:

1. There are several problems (Appendix II) in obtaining a completely rigorous theory expressing a relationship between electron emission and adsorbed atom evaporation in an externally dispensed system. Even to adhere experimentally to the assumptions needed to derive such a relation is quite difficult.

   In an internally dispensed system, a good case may be made for the non-existence of a monolayer thin-film emitter. In order that an internally dispensed cathode maintain exactly a monolayer coverage, the rate of production of the activator, the rate of its transport to the emitting surface, the rate of surface migration, and the rate of evaporation all must be equal. The probability that this occurs in a dispenser cathode is extremely small. Also, the probability that one rate-determining mechanism predominates over the relatively wide range of temperatures over which the measurements were made is unlikely also. The mechanism by which an activator reaches and covers the emitting surface is complicated and can be described at best only qualitatively.

   The exception to this case is that of external dispensing, where the arrival rate is equal to the evaporation rate and a monolayer coverage may be maintained. However, in conventional dispenser type cathodes, there is considerable evidence to indicate that a true monolayer is non-existent.

2. Since the cathode surface is not a uniform monolayer but certainly must vary considerably in the amount of

activator present, the emission constants are affected and may be used as an indication of the relative degree of surface coverage by the activator. The value of the temperature dependence of the work function α is normally the order of 5×10^{-4} ev/^{o}K. Values an order of magnitude higher may result from a non-uniform surface or errors in emission measurement. Procedures are described which may be used to eliminate the latter and thus give some measure of the surface coverage.

SECTION VI
REFERENCES

1. A. H. W. Beck, Proceedings of I.R.E., Vol. 106, Part B, No. 28, pp. 372-390 (1959).

2. K. H. Kingdon and I. Langmuir, Phys. Rev., 21, p. 380 (1923).

3. W. H. Brattain and J. A. Becker, Phys. Rev., 43, p. 428 (1933).

4. A. L. Reimann, Thermionic Emission, Chapman and Hall Ltd., London (1934).

5. E. S. Rittner, R. H. Ahlert, and W. C. Rutledge, J. of App. Phys., 28, pp. 156-166 (1957).

6. W. C. Rutledge and E. S. Rittner, J. of App. Phys., 28, pp. 167-173 (1957).

7. I. Langmuir, J. of Am. Chemical Soc,, 54, pp. 2798-2832 (1932).

8. J. B. Taylor and I. Langmuir, Phys. Rev., 44, pp. 423-458 (1933).

9. E. B. Hensley, J. of App. Phys., 32, pp. 301-308 (1961).

10. C. J. Jansen and R. Loosjes, Philips Research Reports, 8, p. 81 (1953).

11. D. A. Wright, Proceedings I.E.E., Vol. 100, Part III, pp. 125-142 (1953).

12. P. M. Marchuk, Trudy Inst. Fiz Ak Nank Ukraine, No. 7, pp. 17-23 (1956).

13. I. Langmuir and K. H. Kingdon, Proc. Roy. Soc., A 107, p. 61 (1925).

14. L. S. Nergaard, RCA Review, 20, pp. 191-204 (1959).

15. V. L. Stout, Proc. 4th National Conference on Tube Techniques, 1958, New York University Press, p. 178 (1959).

16. H. F. Webster, J. of App. Phys., 32, p. 1802 (1961).

17. P. Schwarzhopf and R. Kieffer, Refractory Hard Metals, MacMillan Co., New York (1953).

18. W. B. Nottingham, Handbuch der Physik, Vol. XXI, Thermionic Emission, Springer-Verlag, Berlin (1956).

19. W. B. Nottingham, Report on the Seventeenth Annual Conference on Physical Electronics, M. I. T., March 1957.

20. J. H. Affleck, Electro Chemical Society Meeting (May 1959).

21. P. P. Coppola, Rev. Sci. Inst., 31, pp. 137-143 (1960).

22. E. S. Rittner, W. C. Rutledge, R. A. Ahlert, J. of App. Physics, 28, pp. 1468-1473 (1957).

23. H. Huber and J. Freytag, LeVide, 54, p. 310 (1954).

24. A. I. Mel'nikov et al, Radiotekhnika i elektronika, No. 3, pp. 322-328 (1958).

25. A. S. Eisenstein, H. John, and J. H. Affleck, J. of App. Phys., 24, pp. 631-632 (1953).

26. P. M. Marchuk, Radio Engr. & Electronics, Vol. 2, No. 12, p. 13 (1957).

27. R. Levi, J. of Appl. Phys., 26, p. 639 (1955).

28. I. Brodie and R. O. Jenkins, J. of App. Phys., 27, pp. 417-418 (1956).

29. C. Herring and M. H. Nichols, Review of Modern Physics, 21, pp. 185-220 (1949).

30. W. R. Ferris, RCA Review, 10, p. 134 (1949).

31. L. Malter, Phys. Rev., 50, p. 48 (1936).

32. P. P. Coppola and R. C. Hughes, Proc. of I.R,E., 44,. pp. 35-59 (1956).

SECTION VII
PERSONNEL

The personnel listed below contributed to the investigation discussed in this report.

J. H. Affleck	-	Power Tube Department
H. J. Beattie	-	Materials & Processes Laboratory, Large Steam Turbine-Generator Department
J. P. Bianchi	-	Power Tube Department
W. T. Boyd	-	Power Tube Department
A. M. Davis	-	Materials & Processes Laboratory, Large Steam Turbine-Generator Department
Dr. C. J. Guare	-	Analytical & Physical Chemistry Section, General Engineering Laboratory
Dr. N. J. Hawkins	-	Power Tube Department
Dr. A. O. Jensen	-	Power Tube Department
A. J. Kiesler	-	Research Laboratory
Dr. A. E. Powers	-	Power Tube Department
B. Tamanian	-	Materials & Processes Laboratory, Large Steam Turbine-Generator Department
Dr. R. P. Wellinger	-	Power Tube Department

SECTION VIII
PUBLICATIONS

Publications under total or partial sponsorship of this investigation are listed below.

A. REPORTS

1. Air Force Contract No. AF19(604)-4093, Scientific Report No. 1, ARCRC-TN-58-372.

2. Air Force Contract No. AF19(604)-4093, Scientific Report No. 2, AFCRC-TN-59-104.

3. Air Force Contract No. AF19(604)-4093, Scientific Report No. 3, AFCRC-TN-59-150.

4. Air Force Contract No. AF19(604)-4093, Scientific Report No. 4, AFCRC-TN-59-367.

5. Air Force Contract No. AF19(604)-4093, Scientific Report No. 5, AFCRC-TN-59-757.

6. Air Force Contract No. AF19(604)-4093, Scientific Report No. 6, AFCRC-TN-60-104.

7. Air Force Contract No. AF19(604)-4093, Scientific Report No. 7, AFCRC-TN-60-183.

8. Air Force Contract No. AF19(604)-4093, Scientific Report No. 8, AFCRC-TN-60-576.

9. Air Force Contract No. AF19(604)-4093, Scientific Report No. 9, AFCRL-TN-60-976.

10. Air Force Contract No. AF19(604)-4093, Scientific Report No. 10, AFCRL-TN-60-1155.

11. Air Force Contract No. AF19(604)-4093, Scientific Report No. 11, ARCRL-140.

12. Air Force Contract No. AF19(604)-4093, Scientific Report No. 12, AFCRL-501.

13. Air Force Contract No. AF19(604)-4093, Scientific Report No. 13, AFCRL-771.

14. Air Force Contract No. AF19(604)-4093, Scientific Report No. 14, AFCRL-1114.

15. Air Force Contract No. AF19(604)-4093, Scientific Report No. 15, AFCRL-62-110.

16. Air Force Contract No. AF19(628)-279, Scientific Report No. 1, AFCRL-62-182.

17. Air Force Contract No. AF19(628)-279, Scientific Report No. 2, AFCRL-62-513.

18. Air Force Contract No. AF19(628)-279, Scientific Report No. 3, AFCRL-62-755.

19. Air Force Contract No. AF19(628)-279, Scientific Report No. 4, AFCRL-63-11.

B. CONFERENCE PAPERS

1. "Thin Film Emitters on Refractory Substrates," by J. H. Affleck. Published in Advances in Tube Techniques I, Pergamon Press, 1961.

2. "Properties of Several Dispenser Cathodes," by J. H. Affleck, Published in Report on Twenty-Second Annual Conference on Physical Electronics, Massachusetts Institute of Technology, March 1962.

3. "The Properties Required for High Current Density Cathodes," by J. H. Affleck. To be published in Advances in Tube Techniques II, Pergamon Press, 1963.

SECTION IX
ACKNOWLEDGEMENTS

A number of people in the Power Tube Department have contributed to this program. In addition to those listed under PERSONNEL, the author wishes to express his appreciation to Dr. N. J. Hawkins for many helpful comments and suggestions, to Mrs. C. B. Hutchinson for the preparation of the reports throughout this program, and to L. C. Lofgran, S. J. Nowicki, and Mrs. Anna Maratta for the fabrication, construction, and processing of the experimental tubes. Also, the encouragement and support of J. H. Bloom of the Air Force Cambridge Research Laboratories is gratefully acknowledged.

APPENDIX I

THE PROPERTIES REQUIRED FOR HIGH CURRENT DENSITY CATHODES*

J. H. Affleck

*This material was presented at the Sixth National Conference on Tube Techniques held during September 1962 and is to be published in the Advances in Tube Techniques, Pergamon Press.

THE PROPERTIES REQUIRED FOR HIGH CURRENT DENSITY CATHODES

by

J. H. Affleck
Power Tube Department
Schenectady, N. Y.

1
THE PROPERTIES REQUIRED FOR HIGH CURRENT DENSITY CATHODES*

The performance of many electron tubes could be improved considerably if high current densities could be obtained reliably from the cathode. It is the purpose of this analysis to examine the properties that an emitter must have in order to qualify for applications where current densities of 1, 10, 20 and even 100 a/cm^2 might be used.

Basically two questions must be answered:

1. What are the limitations of the presently known cathode systems?
2. What properties are necessary for a cathode to supply high current densities?

Before examining the limitations of known systems, it should be pointed out that the electron emission of a dispenser cathode originates from a complex surface. It is composed of alkaline earth oxides, thin films of the alkaline earth metal and/or oxide, and even the substrate itself. In order to achieve the desired operating characteristics, it is necessary to maintain a stable, uniform surface. There are at least four important factors involved in providing such a surface.

1. The production of the barium.
2. The transport of the barium through the pores whether by Knudsen flow and/or surface migration.
3. The diffusion of barium over the cathode surface.
4. The evaporation of barium from the surface.

Each of these factors is a rate process which is temperature dependent and it is highly improbable that each process has exactly the same rate at a given temperature necessary to maintain a monolayer coverage of barium on the cathode surface. If one or more of these processes proceeds at a much greater rate than the others, the surface coverage θ may be either greater or less than unity. For $\theta > 1$, the surface has many layers of barium and the thermionic properties are not necessarily characteristic of barium adsorbed on a refractory surface, but is more similar to barium itself or a composite surface of BaO/Ba. The oxide may form simply by the adsorption of a monolayer of oxygen which at 10^{-8} Torr requires only a few seconds. For $\theta < 1$, the emis-

*This work was supported by the Air Force Cambridge Research Laboratories under Contract No. AF19(628)-279.

sion originates from a "patchy" surface which is reflected in the values obtained for the emission constants as well as in poor performance.

Although Wright,[1] Beck,[2] and Haas[3] have examined some of the properties and limitations of existing thermionic emitters, a more critical examination of the various properties of these systems is needed. There are several references[1, 2, 3, 4] which describe the various cathode systems and their emission properties. Reviewing a few of these systems, it is of interest to note that the best d-c emission data[5] indicates that the effective work function of a well activated oxide coated cathode is:

$$\phi = 1.2 + 4 \times 10^{-4} T \text{ ev.}$$

Cathodes of this type are usually found in tubes where elaborate precautions against contamination and very clean techniques are used.

In most commercial tubes and in many experimental investigations,[6] the oxide cathode has been found to be less active and the work function is consequently higher. A typical value is:

$$\phi = 1.35 + 4 \times 10^{-4} T \text{ ev.}$$

The nickel matrix or bariated nickel[2] cathode has an even higher work function:

$$\phi = 1.76 + 1.4 \times 10^{-4} T \text{ ev.}$$

The "L" cathode,[7] containing (BaSr)O, has emission properties described by:

$$\phi = 1.68 + 3.24 \times 10^{-4} T \text{ ev.}$$

The work function of the barium aluminate impregnated cathode[8] is reported to be:

$$\phi = 1.53 + 5.78 \times 10^{-4} T \text{ ev.}$$

An improved version containing barium calcium aluminate[9] has a work function of:

$$\phi = 1.67 + 3.2 \times 10^{-4} T \text{ ev.}$$

A number of other systems have been examined[10] that also have work functions in this range. Several of these systems are listed in Table I together with those already cited.

Table I - Work Functions of Several Cathode Systems

Systems	$\phi(ev) = \phi_o + \alpha T$	ϕ at 1250°K
BaO on Ni[5, 6]	$1.2 + 4.0 \times 10^{-4} T$	1.70
	$1.35 + 4.0 \times 10^{-4} T$	1.85
Barium-Nickel[2]	$1.76 + 1.4 \times 10^{-4} T$	1.94
"L" Cathode[7]	$1.68 + 3.24 \times 10^{-4} T$	2.09
Barium Calcium Aluminate (pressed)[10]	$1.7 + 3.2 \times 10^{-4} T$	2.12
Barium Aluminate (impregnated)[8]	$1.53 + 5.78 \times 10^{-4} T$	2.25
Barium Calcium Aluminate (impregnated)[9]	$1.67 + 3.2 \times 10^{-4} T$	2.07
$W + Ba_2SiO_4 + ZrH_2 + CaCO_3$[11, 12]	$1.85 + 2.2 \times 10^{-4} T$	2.13
$W + Ba_2TiO_4 + Al$[11, 12]	$1.78 + 3.4 \times 10^{-4} T$	2.20
$Ta + Ba_2TiO_4 + Al$[11, 12]	$2.15 + 5.8 \times 10^{-5} T$	2.22

The emission capabilities and the evaporation rates of these various systems may be compared as shown in Figure 1. It is clear that the oxide coated cathode is the most efficient and that the dispenser cathodes are less efficient in varying degrees. Progress is being made to improve the efficiency of the dispenser system as indicated by the relative position of the barium orthosilicate cathode with the barium oxide cathode.

However, to make a meaningful evaluation of the limitations of these systems, not only must the emission characteristics be compared but also consideration must be given to such parameters as evaporation rate, heater power, joule heating of the coating, electron cooling, and operating temperature. Several of these parameters are determined and listed in Tables II through VI. The first system considered is a well activated oxide coated cathode (Table II). The properties of the bariated nickel cathode, the barium aluminate (impregnated) cathode, the barium calcium aluminate cathode and the barium orthosilicate cathode are listed in Tables III, IV, V and VI, respectively.

In these tables, the saturated emission density, the effective work function, and the cathode temperature are listed in the first three columns respectively. (These values are determined from a plot of the work function data in Table I as shown in Figure 2.) The evaporation rate is given in the fourth column. The next five columns are concerned with the power sources and losses in the cathode. The power sources include the heater power, P_h, and the joule heating, P_j, of the coating by the I_s^2R losses in the coating. In order to maintain an equilibrium temperature, these sources are balanced by the power losses: i.e. by conduction, radiation, and electron cooling. The loss by conduction, P_c, can be significant but for this discussion will be neglected. Therefore, the input power is lost by radiation, P_r, and electron cooling, P_{ec}. If no current is being drawn from the cathode, then the heater power is dissipated only by radiation which can be determined from the cathode temperature and Stefan's Law. Although a value of 0.3 was assumed for the total emissivity, this value may be lower in some cases but certainly is not higher. The heater power must then be greater than the radiated power. The figures for the heater power are a minimum value while those for the power loss by radiation are a maximum value.

The power lost by electron cooling, P_{ec}, is given by:

$$P_{ec} = I_s \phi + 1.72 \times 10^{-4} I_s T$$

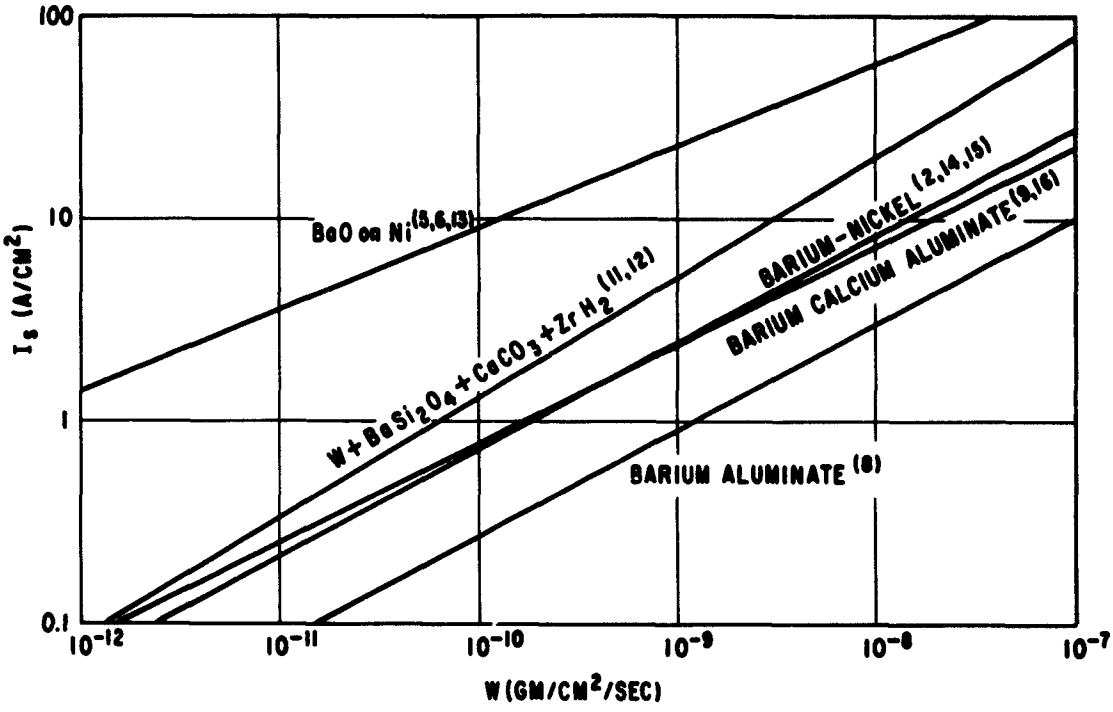

Figure 1 - Current Density versus Evaporation Rate

Table II - Properties of an Oxide Coated Cathode[4, 5, 6, 13]
($\phi = 1.2 + 4 \times 10^{-4} T$)

I_s (a/cm^2)	ϕ (ev)	T (^oK)	W_2 (gm/cm^2/sec)	P_h (watts/cm^2)	$P_j = I_s^2 R$ ($R = 1$ ohm/cm^2) (watts/cm^2)	P_c	P_r (watts/cm^2)	P_{ec} (watts/cm^2)
1	1.60	1000	5.0×10^{-13}	> 1.7	1	-	1.7	1.77
10	1.66	1160	1.4×10^{-10}	> 3.1	100	-	3.1	18.6
20	1.69	1220	8.0×10^{-10}	> 3.8	400	-	3.8	38.0
50	1.72	1300	7.0×10^{-9}	> 4.8	2500	-	4.8	97.2
100	1.75	1380	4.5×10^{-8}	> 6.0	10^4	-	6.0	198.7

Table III - Properties of the Bariated Nickel Cathode[2, 14, 15]
($\phi = 1.76 + 1.4 \times 10^{-4} T$)

I_s (a/cm^2)	ϕ (ev)	T (^oK)	W ($gm/cm^2/sec$)	P_h ($watts/cm^2$)	P_j ($watts/cm^2$)	P_c	P_r ($watts/cm^2$)	P_{ec} ($watts/cm^2$)	t_m (sec)	t_d (sec)
1	1.92	1180	2.3×10^{-10}	>3.3	-	-	3.3	2.12	335	19.2
10	1.94	1340	1.6×10^{-8}	>5.4	-	-	5.4	21.7	4.8	7.4
20	1.95	1390	6.0×10^{-8}	>6.4	-	-	6.4	43.8	1.28	5.6
50	1.96	1425	1.2×10^{-7}	>7.0	-	-	7.0	110.3	0.64	4.5
100	1.98	1540	1×10^{-6}	>9.5	-	-	9.5	224.5	7.7×10^{-2}	2.8

Table IV - Properties of the Barium Aluminate (Impregnated) Cathode[8]
($\phi = 1.53 + 5.78 \times 10^{-4}\ T$)

I_s (a/cm^2)	ϕ (ev)	T (^oK)	W_2 ($gm/cm^2/sec$)	P_h ($watts/cm^2$)	P_j ($watts/cm^2$)	P_c	P_r ($watts/cm^2$)	P_{ec} ($watts/cm^2$)	t_m (sec)	t_d (sec)
1	2.32	1400	1.2×10^{-9}	> 6.5	-	-	6.5	2.56	64	2.4
10	2.45	1660	1.2×10^{-7}	> 13.0	-	-	13.0	27.4	0.64	0.83
20	2.53	1760	4.0×10^{-7}	> 16.5	-	-	16.5	57.2	0.19	0.65
50	2.61	1880	1.5×10^{-6}	> 21.0	-	-	21.0	146.7	5.1×10^{-2}	0.45
100	2.67	2000	3.0×10^{-6}	> 27.0	-	-	27.0	301.4	2.6×10^{-2}	0.34

Table V - Properties of the Barium Calcium Aluminate Cathode[9, 16]
($\phi = 1.67 + 3.2 \times 10^{-4}\ T$)

I_s (a/cm^2)	ϕ (ev)	T (^oK)	W (gm/cm^2/sec)	P_h (watts/cm^2)	P_j (watts/cm^2)	P_c	P_r (watts/cm^2)	P_{ec} (watts/cm^2)	t_m (sec)	t_d (sec)
1	2.07	1260	1.68×10^{-10}	> 4.2	-	-	4.2	2.29	460	2.85
10	2.13	1455	1.8×10^{-8}	> 7.5	-	-	7.5	23.8	4.3	1.04
20	2.16	1520	7.3×10^{-8}	> 9.0	-	-	9.0	48.5	1.06	0.78
50	2.18	1605	1.05×10^{-7}	> 11.0	-	-	11.0	122.8	0.735	0.57
100	2.21	1700	1.46×10^{-6}	> 14.0	-	-	14.0	250.3	0.053	0.395

Table VI - Properties of Barium Orthosilicate Cathode[11, 12]
($\phi = 1.85 + 2.2 \times 10^{-4}$ T)

I_s (a/cm^2)	ϕ (ev)	T (^oK)	W (gm/cm^2/sec)	P_h (watts/cm^2)	P_j (watts/cm^2)	P_c	P_r (watts/cm^2)	P_{ec} (watts/cm^2)	t_m (sec)	t_d (sec)
1	2.13	1280	6.0×10^{-11}	> 4.4	-	-	4.4	2.34	1280	4.3
10	2.17	1470	3.0×10^{-9}	> 8.0	-	-	8.0	24.2	25.6	1.8
20	2.19	1540	1.1×10^{-8}	> 9.5	-	-	9.5	49.1	7.0	1.3
50	2.21	1620	4.5×10^{-8}	> 12.0	-	-	12.0	124.4	1.7	1.0
100	2.22	1700	1.2×10^{-7}	> 14.0	-	-	14.0	251.3	0.64	0.78

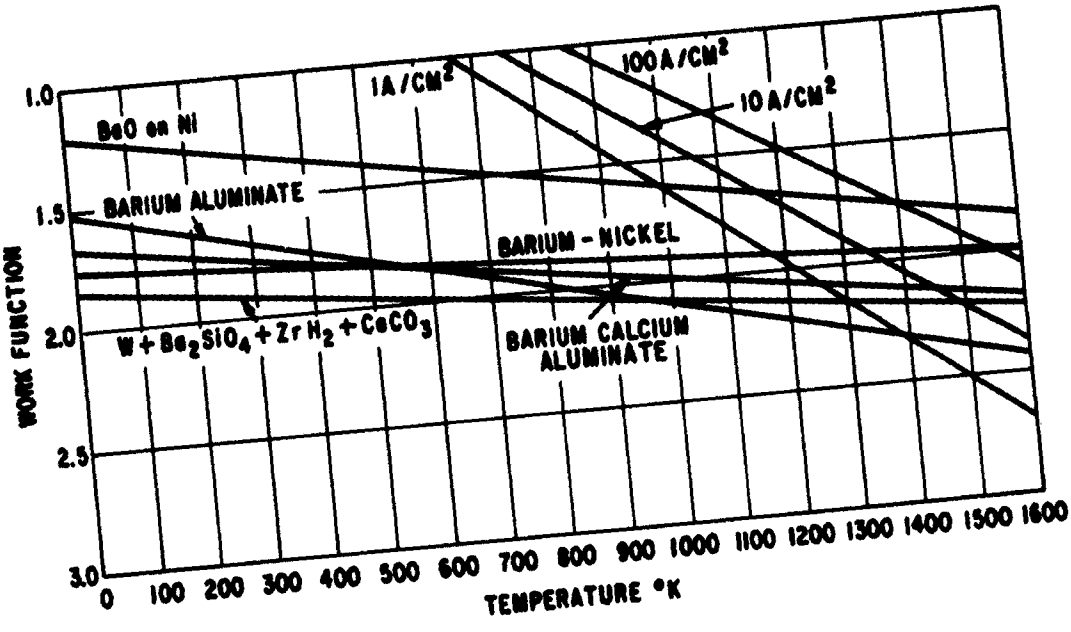

Figure 2 - Work Function versus Temperature

where I_s is the saturated emission in amperes, ϕ is the effective work function at the temperature $T^{\circ}K$.

Two additional columns have been included in Tables III, IV, V, and VI. One column gives the time in seconds, t_m, to evaporate a monolayer, while the second column lists the time, t_d, for a barium atom to diffuse over a distance equivalent to half the pore separation. The values for t_d have been determined for a path length of 2.5 microns based upon the use of a refractory matrix composed of particles 5.0 microns in diameter. It is clear that the time for evaporating a monolayer must be greater than the time it takes to cover the emitting surface with barium.

Analyzing the information contained in Tables II through VI, a number of interesting observations may be made. The data for a well activated cathode (Table II) indicates that the joule heating in the cathode coating becomes a severe problem at current densities much over 1 a/cm^2. Although thinner and consequently less resistive coatings may be used, the evaporation of emissive material which will in turn affect the life must be considered. Consequently, the maximum d-c current density that an oxide coated cathode may be expected to deliver is about 1 a/cm^2. Under pulsed conditions, however, this figure is much higher since the joule heating, P_j, and electron cooling, P_{ec}, terms are altered by a factor equal to the duty cycle. For a duty cycle of 0.001, the joule heating is correspondingly lowered by this amount which makes much higher current operation possible as shown by Coomes.[17] However, duty cycles greater than 0.001 are frequently used which may limit the maximum pulsed emission density in practical applications.

In a dispenser cathode the emissive coating is very thin and has a very low resistance, consequently the joule heating is also very small and for all practical purposes may be neglected. This makes the electron cooling term more important, for as the current density increases, the electron cooling increases and the cathode temperature is lowered. To maintain the desired emission and cathode temperature, an equivalent amount of power must be supplied to the heater. Most coated heaters cannot be expected to operate above 1800°K which, in turn, limits the cathode temperature to about 1500°K. Therefore, an uncoated heater must be used at higher current densities and necessarily higher cathode temperatures. Even then, the temperature of the heater and its evaporation must not exceed prudent limits in order to assure reasonable lifetimes.

An additional factor to be considered in the case of the dispenser cathodes is the maintenance of a uniform emitting surface. In order to maintain complete coverage of the cathode surface with the emissive material, the rate of evaporation must be such that the time required to evaporate a monolayer of barium from the surface is large compared to the time to replace the barium by surface diffusion. From the values for the evaporation rate at the various temperatures, it is a simple matter to determine the time to evaporate a monolayer, t_m. The time required to cover the surface by surface diffusion, t_d, is estimated using the method of Rittner et al.[7]

When the figures for t_d and t_m are compared, it is apparent that at higher cathode temperatures the time required to evaporate a monolayer is less than the time required to completely cover the surface of the cathode with barium.

It is clear that, on the basis of the systems and assumptions made in this analysis, there are a number of important considerations and limitations in the design of high current density cathodes. To summarize a few of these:

1. The available d-c current density from an oxide coated cathode and a bariated nickel cathode is not much greater than 1 a/cm^2, while for barium aluminate the current density is $\sim$10 a/cm^2. The data for the barium orthosilicate cathode indicates that it is capable of delivering in excess of 20 a/cm^2. These conclusions are based not only on work function, cathode temperature, power losses in coating, and electron cooling but also on the time required to evaporate a monolayer and to obtain maximum surface coverage.

2. Under pulsed conditions, both the oxide and dispenser systems are capable of high current densities. Although the oxide cathode has the advantage of being more efficient, care must be exercised in the choice of duty cycles so as not to produce excessive joule heating of the cathode. The dispenser cathodes may be limited by the life of the heater. Excessive heater temperature and correspondingly short heater life may prevent the attainment of 100 a/cm^2.

3. Uncoated heaters should be used for higher current density requirements; even then the operating temperature of the heater may be too high to give adequate life.

4. The evaporation of these cathode systems must also be considered. It is difficult to evaluate fully the effect that evaporation will have on tube performance except under actual operating conditions. Evaporated deposits may not be harmful to a beam

tube but may be detrimental to a close spaced triode or tetrode. The consequences of the evaporation rate must be examined for each application.

5. The particle size of the refractory material has been shown to be important in maintaining a uniform emitting surface. For the purpose of the calculations, a particle size of five microns was used. It would seem that the particle size should not be much larger than this value. Perhaps large particles could be used if the rate of surface diffusion were increased, however, there is little information available on the diffusion of barium over various surfaces.

REFERENCES

1. Wright, D. A., "A Survey of Present Knowledge of Thermionic Emitters," Proc. Inst. of Elect. Engineers, vol. 100 (pt. 3), p. 125, 1953.
2. Beck, A. H. W., "High-Current-Density Thermionic Emitters: A Survey," Proc. Inst. of Elect. Engineers, vol. B106, p. 372, 1959.
3. Haas, G. A., "Thermionic Electron Sources," Naval Research Laboratory, Report 5657, 1961.
4. Stout, V. L., "Dispenser Cathodes," General Electric Research Laboratory, Report No. 58-RL-2136.
5. Stout, V. L. and Beggs, J. E., Private Communication.
6. Sparks, L. L. and Philipp, H. R., "A Retarding Potential Method for Measuring Electrical Conductivity of Oxide-Coated Cathodes," J. of Applied Physics, vol. 24, pp. 453-461, 1953.
7. Rittner, E. S. et al, "Studies on the Mechanism of Operation of the L Cathode. I.," J. of Applied Physics, vol. 28, pp. 156-166, 1957.
8. Rittner, E. S. et al, "On the Mechanism of Operation of the Barium Aluminate Impregnated Cathode," J. of Applied Physics, vol. 28, p. 1468, 1957.
9. Levi, R., "Improved 'Impregnated Cathode'," J. of Applied Physics, vol. 26, p. 639, 1955.
10. Coppola, P. P. and Hughes, R. C., "A New Pressed Dispenser Cathode," Proc. IRE, vol. 44, p. 351, 1956.
11. Affleck, J. H., "Properties of Several Barium Dispenser Cathodes," Paper Presented at Twenty-Second Annual Conference of Physical Electronics, M. I. T., 1962.
12. Affleck, J. H., "Investigation of Various Activator-Refractory Substrate Combinations," Air Force Contract No. AF19(604)-4093, Scientific Reports No. 14 and 15 (AFCRL 1114 and AFCRL-62-110).
13. Gibbons, M. D. and Stout, V. L., "Evaporation Rate of Oxide Cathodes of X-ray Emission Spectrometry," Bull. Amer. Phys. Soc., vol. 3, no. 4, 1958.
14. Fane, R. W., "A Sintered Nickel Matrix Cathode," British J. of App. Phys., vol. 9, no. 4, p. 149, 1958.
15. Jenkins, R. O. and Trodden, W. G., "Evaporation from Barium Nickel Matrix Cathodes," J. of Elec. and Control, vol. 11, no. 1, p. 1, 1961.

16. Brodie, I., Jenkins, R. O., and Trodden, W. G., "Evaporation of Barium from Cathodes Impregnated with Barium-Calcium-Aluminate," J. of Elec. and Control, vol. 6, p. 149, 1959.

17. Coomes, E. A., "Pulsed Properties of Oxide Cathodes," J. of Applied Physics, vol. 17, p. 647, 1946.

APPENDIX II

CONCLUSIONS CONCERNING THE LANGMUIR APPROACH*

Dr. N. J. Hawkins

Langmuir's essentially thermodynamic approach led to the calculated "S-curves" for the electron emission of tungsten in equilibrium with cesium vapor at various temperatures.[1] These curves have not only been accurately confirmed experimentally within the limits of his original calculations, but also calculated S-curves at cesium arrival rates many orders of magnitude higher have recently been confirmed experimentally.[2]

An even more remarkable result of this approach is the experimental verification of the calculated contact potential variation with θ (Reference 1, Figure 14, p. 437). "On-the-nose" agreement was obtained up to slightly less than one-half a monolayer coverage for cesium-on-tungsten with cesium arrival rates varying by two orders of magnitude. Divergence between calculation and experiment began to occur for $\theta > 0.5$, with experimental values always lower than calculated. The measured contact potential goes through a maximum at $\theta = 0.67$ and then declines. This maximum was not predicted by the calculations which indicate, instead, a monotone increasing dependence on θ.

It is important to note that the significant predictions of contact potentials and emission characteristics were calculated from evaporation rate data by methods Langmuir described in an earlier paper.[3] In this paper, Langmuir rigorously derived an explicit relation between the equilibrium evaporation rate, which contained, among other things, the dipole moment. This is presumed to be the dipole moment that one

*These paragraphs are "thoughts" since Scientific Reports No. 1 and No. 2 under Contract No. AF19(604)-4093 and approximately 4-1/2 years of emission research were carried on by others in connection with cesium vapor thermionic converters.

needs to evaluate the contact potential. In an electrical double layer, it can be shown that the contact potential difference between the film and pure metal substrate is given by $V_2 = 2\pi M \sigma_1 \theta$. If the film, in effect, is more complicated than a simple double layer, a different type of relation may have to be found.

Using Langmuir's equation numbers from reference 3, the evaporation rate (rigorously) is given by:

$$\ell n\, \nu_a = \ell n \frac{\theta}{1-\theta} + \frac{1}{1-\theta} + \frac{1}{\sigma_1 kT} \int \frac{dF'}{\theta} \qquad (1)$$

where ν_a = evaporation rate

θ = number of monolayers

σ_1 = concentration of a unit monolayer in atoms per cm^2.

F' = contribution of long-range repulsive forces to the total spreading force of the adsorbed film (Equations (2) and (3))

k, T = the Boltzmann constant and absolute temperature.

Equation (1) is obtained from Equation (2), which is:

$$\ell n\, \nu_a = \frac{1}{\sigma_1 kT} \int \frac{dF}{\theta} \qquad (2)$$

where dF is the derivative of the total spreading force of the adsorbed film (which considers both the powerful short-range forces, which can be evaluated in a straight-forward manner, and the long-range forces, which depend on the dipole moment, and are not so simply evaluated).

$$F = \frac{\sigma_1 kT\theta}{1-\theta} + F' \qquad (3)$$

Theoretically, one can derive for F' that:

$$F' = 3.338\, M^2 \sigma^{5/2} + (1.531 \times 10^{-5})\, \sigma^2\, T^{1/3}\, M^{4/3}\, I \qquad (4)$$

where σ, the actual surface concentration, is given by $\theta\sigma_1$; and I, the rather formidible integral, is given by:

$$I = \exp(u_2^3) \int_{u_2}^{u_o} \exp(-x^3)\, dx \qquad (5)$$

with $u_o = 2.181 \times 10^5 M^{2/3} T^{-1/3} \sigma_1^{1/2}$

$$u_2 = 2.181 \times 10^5 M^{2/3} T^{-1/3} \sigma_1^{1/2} \theta^{1/2}$$

$$= u_o \theta^{1/2} .$$

Experimentally, one finds, from measured evaporation data, that:

$$F' = (0.1172\,\theta^2 - 0.078\,\theta^3)\,T + 2215\left[\ln(1+\beta\theta) - \frac{\beta\theta}{1+\beta\theta}\right] \qquad (6)$$

with $\beta = 0.714$, an integration constant chosen to make $F' = 0$ at $\theta = 0$.

This relation is obtained by expressing Taylor's evaporation rate data in the form of an Arrhenius equation in such a manner that A and B are only functions of θ.

Langmuir then obtains the dipole moment by equating the theoretical equation (Equation (4)) to the equation representing the experimental data (Equation (6)) and solves the equations for M at various θ and T. He found that M had a significant dependence on θ.

At a temperature of 800°K and $\theta = 0$, M had the value of 16.16 debeye units. We found that this value is comparable to 16.23 debeye units if we took 1.69Å as the cesium ion radius,[4] and a separation of the ion-electron image charge of twice this distance.

The M that Langmuir obtained from his equations, however, decreased rather rapidly with θ; e.g., it was 8.28 at $\theta = 0.5$ and about 7.25 at $\theta = 0.67$, the point at which the maximum in the contact potential is found to occur.

We began our extension* of the Langmuir work with the thought that a maximum (or at least a plateau) in the V_c versus θ curve can be explained - and indeed surely must occur at some point in θ - on the basis of the following considerations. One can only expect a purely ion-image attraction between a sorbed atom and a substrate when the ionization potential of the sorbed atom is less than or equal to the electron affinity (work function) of the substrate. As the substrate builds up positive ions, its now composite electron affinity (work function) decreases, thus leaving less and less of a basis for an attractive force, particularly if the sorbed particles have significant mobility. Thus, one must look elsewhere for surface binding energy when the composite substrate electron affinity is 3.87 volts or less (the ionization potential of cesium). Langmuir, in effect, took the view that evaporation was related to the "net" dipole moment which the atom felt as the result of a force = $3M^2/2r^4$. This "net" dipole moment, M, is identically the same as that which an electron would feel if it evaporated (emitted). Thus, Langmuir took the pragmatic view that, regardless of the detailed nature of M and its relation to the "structure" of the film, it could be obtained from evaporation rate data. Furthermore, he in effect implied that the same force equations govern both phenomena (emission and evaporation) and the only significant force in the equation of state was that of repulsion between two parallel, similarly oriented dipoles. Nowhere in these papers did he pursue the question as to just why this dipole moment decreased with θ.

Although there are approaches to the understanding of this question, they lead either to a too difficult experiment to prove the model or to a too difficult calculation to predict the final details of the facts available. Langmuir was wise in his selection of a stopping point.

We tried to approach, which, in effect, added a second force in the virial equation of opposite sign to allow for attraction between neutral atoms as the result of London dispersion forces.[5] A well-known equation,

*Scientific Reports No. 1 and No. 2, Contract AF19(604)-4093

derived by F. London, for the interaction energy between two atoms resulting from dispersion forces is:

$$U_D = -\frac{3}{4} \frac{h \nu_o \alpha^2}{r^6} \tag{7}$$

where h = Planck's constant

ν_o = a characteristic frequency of the atom

α = polarizability of the atom.

London further showed that for many gases, ν_o is related to the ionization potential. Then the second force, f_2, is:

$$f_2 = \frac{\partial \nu_o}{\partial r} = \frac{9}{2} h \nu_o \alpha^2 \left(\frac{1}{r^7}\right) \tag{8}$$

This attractive force is about two orders of magnitude less than the force of repulsion between two parallel dipoles per atom (ion) pair at a distance of 5.44Å (one cesium atom diameter).

We tried rederiving the Langmuir equations, assuming that we could separate the total number of sorbed particles into those which are ionized (which were expected to dominate the problem at low values of θ) and those which are essentially neutral (which were expected to increase considerably as θ increased). It was hoped that we could predict the type of deviations and maximum found experimentally in the V_c versus θ curve.[1]

Using this approach, however, one is led rather abruptly to a dead end because one needs to know the surface ionization equilibrium constant for the reaction $Cs = Cs^+ + e^-$ on tungsten. This is a prohibitively difficult constant to obtain experimentally.

The picture that seems to fit most of the facts is that one has relatively fixed dipoles of ions imaged to the surface in such concentration ($\sim\theta = 0.01$) that they form a composite electron affinity surface in the neighborhood of 3.87 volts with the substrate. One also has highly mobile neutrals that cluster about these "active centers" in such a manner that the cluster as a whole is held by attracting dispersion forces (to each

other) thereby: (1) introducing a term of opposite sign into the virial equation; (2) giving, in effect, a smaller measurable dipole moment; (3) providing an easy path for atoms to evaporate (one climbing on top of the cluster); and (4) continual "dispensing" of activator atoms to the ion site. Should this picture be correct, one would expect to find an extremely patchy type of emission because the active sites, initially, are undoubtedly provided by the high work function planes in the substrate.

It is somewhat doubtful that it is worthwhile, with known present-day experimental techniques, to pursue a complete theory of external dispensing of activator atoms - particularly if our cluster model is correct, because this model could be looked upon as almost as much an internally dispersed system as one that is externally dispensed. J. H. Affleck's data on internally dispensed activator systems clearly indicates that there just are not simple relations connecting emission and evaporation rate.

References

1. J. B. Taylor and I. Langmuir, Phys. Rev., 44, p. 438 (1933).

2. J. M. Houston, Proc. of the Round-Table Discussion, Power Information Center Report PIC-ELE-TI 3/3, Univ. of Penna., Appendix F-1, June 1 and 2, 1961.

3. I. Langmuir, J. Am. Chem. Soc., 54, p. 2798 (1932).

4. A. F. Wells, "Structural Inorganic Chemistry," Oxford, p. 70 (1950).

5. F. London. See S. Glasstone, "Theoretical Chemistry," Van Nostrand (1949).

APPENDIX III
X-RAY ANALYSES OF COMPOUNDS

The x-ray analyses of the compounds studied in this report were performed by H. J. Beattie and Alice M. Davis, Materials and Processes Laboratory, Large Steam Turbine-Generator Department, General Electric Company. The appendix includes tabular matter and a list of references noted in the table.

Analyses of Compounds

Spec.No.	Intended Compound	System	Typical Lattice Parameter (Å)	X-Ray Identification*	Abundance**	Calculated Lattice Parameter (Å)
1	$BaAl_4$	Tetragonal	$a = 4.530$ $c = 11.14$	$BaAl_4$ [1][2]	(a)	$a_o = 4.532$ $c_o = 11.192$
				Plus a few unidentified, very weak lines		
2	CrB	Orthorhombic	$a_o = 2.969$ $b_o = 7.858$ $c_o = 2.932$	-CrB [3]	(a)	$a_o = 2.982$ $b_o = 7.836$ $c_o = 2.926$
		Hexagonal	$a_o = 2.972$ $c_o = 3.069$	CrB_2 [4]	(ma)	$a_o = 2.968$ $c_o = 3.061$
				Plus numerous unidentified lines		
3	VB	Orthorhombic	$a = 3.10$ $b = 8.17$ $c = 2.98$	VB [5]	(a)	$a_o = 3.057$ $b_o = 8.056$ $c_o = 2.968$
		Hexagonal	$a_o = 2.998$ $c_o = 3.060$	VB_2 [6]	(mr)	$a_o = 2.994$ $c_o = 3.058$
		BCC	$a_o = 3.04$	V	(r)?	$a_o = 3.023$
				Plus several unidentified weak lines		
4	CbB_2	Hexagonal	$a_o = 3.10$ $c_o = 3.30$	CbB_2 [7]		$a_o = 3.094$ $c_o = 3.286$
				Plus one or two unidentified lines		
5	TaB_2	Hexagonal	$a_o = 3.078$ $c_o = 3.265$	TaB_2 [8]	(a)	$a_o = 3.074$ $c_o = 3.258$
		Orthorhombic	$a = 3.29$ $b = 14.0$ $c = 3.13$	Ta_3B_4 [9]	(vr) (questionable)	
6	TiB_2	Hexagonal	$a_o = 3.028$ $c_o = 3.228$	TiB_2 [10]	Essentially pure	$a_o = 3.030$ $c_o = 3.225$

*Superscripts refer to APPENDIX III references

**(a) = abundant; (m) = medium, moderately; (r) = rare; (v) = very

Analyses of Compounds (cont'd.)

Spec. No.	Intended Compound	System	Typical Lattice Parameter (Å)	X-Ray Identification*	Abundance**	Calculated Lattice Parameter (Å)
7	WB_2	Hexagonal	$a_o = 2.982$ $c_o = 13.87$	W_2B_5 (previously described as WB_2)[11][12]	(a)	$a_o = 2.974$ $c_o = 13.866$
		Tetragonal	$a_o = 3.115$ $c_o = 16.93$	-WB[13]	(a)	$a_o = 3.094$ $c_o = 16.908$
				Plus a few unidentified very weak lines		
8	ZrB_2	Hexagonal	$a_o = 3.169$ $c_o = 3.530$	ZrB_2[14]	(a)	$a_o = 3.168$ $c_o = 3.530$
		FCC	$a_o = 7.408$	ZrB_{12}[15]	(vr)	$a_o = 7.396$
		Hexagonal	$a_o = 3.232$ $c_o = 5.147$	-Zr[16]	(r)?	$a_o = 3.257$ $c_o = 5.128$
				Plus a few unidentified very weak lines		
9	CrSi	Cubic	$a_o = 4.629$	-CrSi[17][18]	(a)	$a_o = 4.628$
				Plus numerous prominent lines that cannot be identified		
10	$CbSi_2$	Hexagonal	$a_o = 4.797$ $c_o = 6.592$	$CbSi_2$[19]	(a)	$a_o = 4.795$ $c_o = 6.587$
		FCC	$a_o = 5.430$	Silicon	(r)	$a_o = 5.422$
				Plus one additional line		
11	$MoSi_2$	Tetragonal	$a_o = 3.20$ $c_o = 7.86$	$MoSi_2$[20]	Pure compound	$a_o = 3.201$ $c_o = 7.847$
12	$TaSi_2$	Hexagonal	$a_o = 4.782$ $c_o = 6.569$	$TaSi_2$[21]	(a)	$a_o = 4.781$ $c_o = 6.566$
				Plus several unidentified very weak lines		
13	$TiSi_2$	Orthorhombic	$a_o = 8.236$ $b_o = 4.773$ $c_o = 8.523$	$TiSi_2$[22]	(a)	$a_o = 8.259$ $b_o = 4.802$ $c_o = 8.552$
				Plus several unidentified weak lines		
14	VSi_2	Hexagonal	$a = 4.571$ $c = 6.372$	VSi_2[23]	(a)	$a_o = 4.573$ $c_o = 6.369$
		FCC	$a_o = 5.430$	Silicon	(a)	$a_o = 5.425$
15	WSi_2	Tetragonal	$a = 3.211$ $c = 7.868$	WSi_2[24]	(a)	$a_o = 3.211$ $c_o = 7.830$
				$WSi_{0.7}$[25]	Questionable (vr)	
				Plus few extra very weak lines		
16	$ZrSi_2$	Orthorhombic	$a_o = 3.69$ $b_o = 14.71$ $c_o = 3.67$	$ZrSi_2$[26]	(a)	$a_o = 3.685$ $b_o = 14.641$ $c_o = 3.661$
		FCC	$a_o = 5.430$	Silicon	(mr)	$a_o = 5.422$
				Plus a few unidentified very weak lines		
17	$BaSi_4$	To date, no work has been done on this system by x-ray diffraction, although Reference 27 cites BaSi, $BaSi_2$ and $BaSi_3$ compounds identified by chemical analysis.		Complicated pattern most of which has not been indexed. However silicon is abundant in this mixture.	(a)	$a_o = 5.432$

*Superscripts refer to APPENDIX III references

**(a) = abundant; (m) = medium, moderately; (r) = rare; (v) = very

References

1. W. B. Pearson, Handbook on Lattice Spacings and Structures of Metals, p. 316 (1958).

2. K. R. Andress, and E. Alberti, Z. Metallk, 27, p. 126 (1935).

3. ASTM Card No. 9-361 (R. Kiessling, Acta Chem. Scand., 3, pp. 595-602, 1949).

4. ASTM Card No. 8-119 (Paretzkin, Polyechnic Inst. of Brooklyn, 1956).

5. H. Blumenthal, J. Am. Chem. Soc., 74, p. 2942 (1952).

6. ASTM Card No. 8-118 (Paretzkin, Polytechnic Inst. of Brooklyn, 1956).

7. ASTM Card No. 8-120 (Paretzkin, Polytechnic Inst. of Brooklyn, 1956).

8. ASTM Card No. 8-115 (Kiessling, Acta Chem. Scand., 3, p. 603, 1949).

9. ASTM Card No. 5-0744 (Kiessling, Acta Chem. Scand., 3, pp. 608-612, 1949).

10. ASTM Card No. 8-121 (Kiessling, Acta Chem. Scand., 4, p. 209, 1950).

11. W. B. Pearson, Handbook of Lattice Spacings and Structures of Metals, p. 910 (1958).

12. ASTM Card No. 6-0243 (Kiessling, Acta Chem. Scand., 1, pp. 893-916, 1947).

13. ASTM Card No. 6-0635 (Kiessling, Acta Chem. Scand., 1, pp. 893-916, 1947).

14. ASTM Card No. 6-0610 (Kiessling, Acta Chem. Scand., 3, p. 90, 1949).

15. ASTM Card No. 6-0590 (B. Post, and F. W. Glaser, J. Metals, 4, p. 631, 1952).

16. ASTM Card No. 5-0665 (Swanson and Fuyat, NBS Circular 539, 2, p. 11, 1953).

17. W. B. Pearson, Handbook of Lattice Spacings and Structures of Metals, p. 562 (1958).

18. R. Kieffer, F. Benesovsky, and H. Schroth, Z. Metallk, 44, p. 437 (1953).

19. ASTM Card No. 8-450 (NBS Circular 539, 8, 1958).

20. ASTM Card No. 5-0749 (W. H. Zachariasen, Z. Phys. Chem., 128, pp. 39-48, 1927).

21. ASTM Card No. 8-53 (NBS Circular 539, 8, 1958).

22. ASTM Card No. 2-1120 (F. Laves, and H. J. Wallbaum, Z. Kri., 101, p. 78, 1939).

23. W. B. Pearson, Handbook of Lattice Spacings and Structures of Metals, p. 856 (1958).

24. W. B. Pearson, Handbook of Lattice Spacings and Structures of Metals, p. 857 (1958).

25. ASTM Card No. 8-350 (Brewer et al, J. Am. Ceram. Soc., 33, pp. 291-294, 1950).

26. ASTM Card No. 6-0566 (American Electro Metal Company, Yonkers, New York).

27. L. Wöhler, and W. Schuff, Z. Anorg. Chem., 209, p. 33 (1932).

APPENDIX IV
THE DETERMINATION OF EVAPORATION RATES BY X-RAY EMISSION SPECTROGRAPHY

J. H. Affleck

A technique has been reported by Gibbons, Stout, and Zemany[1,2] to determine the evaporation rates of elemental barium, strontium, and calcium from thermionic emitters by use of x-ray emission spectrography. This method is based upon the principle that the characteristic x-ray line spectra of an element can be excited when the element is exposed to a high intensity x-ray beam. The elements may be identified by the wavelength of their spectral lines and their concentration from the intensities of the line. Since x-ray emission spectrography is well suited to the analysis[3] of microgram deposits elements, the technique provides a means of detecting monolayers of evaporant.

In practice,* a chromium target x-ray tube is operated at a relatively high output (45 ma, 50 kv) to provide a source of x-rays with a range of wavelengths of sufficient intensity to excite the characteristic K and L spectra of the elements in the sample being analyzed. The characteristic radiations emitted by the elements in the sample are diffracted at the Bragg angle (θ) by a suitable crystal (LiF) with a known interplanar spacing, d. The radiation then passes, in a helium atmosphere, through a 0.020-inch collimator and is finally detected by a proportional counter. The wavelength of the characteristic radiation is determined by solving Bragg's law for λ.

$$n\lambda = 2d \sin \theta \qquad (1)$$

Since each element has a characteristic spectra, then λ may be identified as having originated from a particular element. The intensity of the radiation above the background is directly proportional to the amount

*All x-ray emission spectrographic analyses were made by Mr. B. Tamanian, Materials and Processes Laboratory, General Electric Company.

of the element in the specimen. With commercially available x-ray equipment, the counting rates range from tens of counts per second per microgram for elements like copper to tenths of a count per second for the most unfavorable element within the range of the apparatus. The precision of a particular measurement has been shown to be that expected by statistical theory.[4]

The application of this technique to the measurement of evaporation rates of thermionic emitters requires a special tube (Figure 1) in which a number of collectors are mounted on a track so that they may be manipulated, one at a time, into position over the cathode. By operating the cathode at various temperatures for known time intervals, the evaporation products from the emitter are deposited on each of the collectors. After a series of evaporations, the collectors are examined by x-ray emission spectrography. In order to measure the deposit on the collectors, the tube must be cracked open and the collectors carefully removed and placed in the sample holder of the x-ray spectrograph.

In the case of barium, the intensity of the barium L_α line is determined in counts per second after subtracting the background measured at a nearby wavelength. The net count is directly proportional to the amount of barium present. To convert counts per second to quantity of material deposited per second, it is necessary to make a calibration curve similar to that shown in Figure 2 and determine the slope or calibration factor. This curve is obtained by depositing known amounts of barium as a salt (barium acetate) from a solution onto aluminum foil disks similar to those used for the collectors. When the solvent has evaporated, a small known amount of barium is left on the aluminum foil. The counting rate and background are measured and the difference is plotted versus the quantity of barium as the calibration curve. The method is sufficiently sensitive for detecting quantities of barium in the range of 0.05 to 100 micrograms.

The quantity of barium deposited on the collector must be corrected for the geometrical configuration,[5] and the areas of the emitter in order to arrive at the quantity of material evaporated from a unit area in a unit time at a given temperature.

Repeating this procedure for several temperatures, enough data may be obtained to plot the logarithm of the evaporation rate versus the reciprocal of the temperature, as in Figure 3. This data can be expressed in an equation of the Arrhenius form:

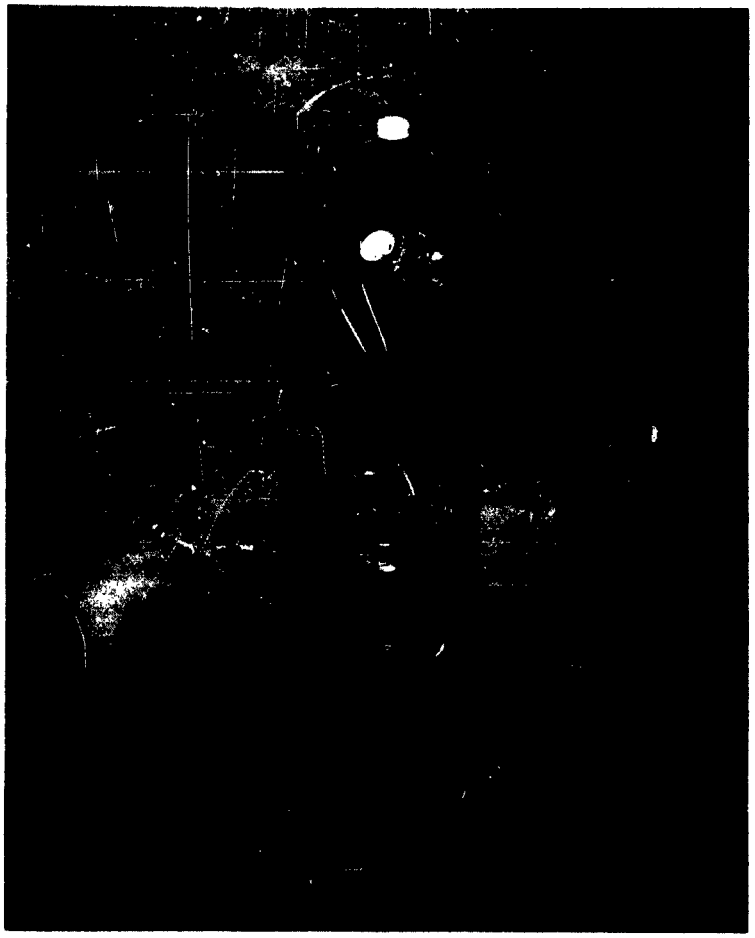

Figure 1 - Tube Used for Determining Evaporation Rates

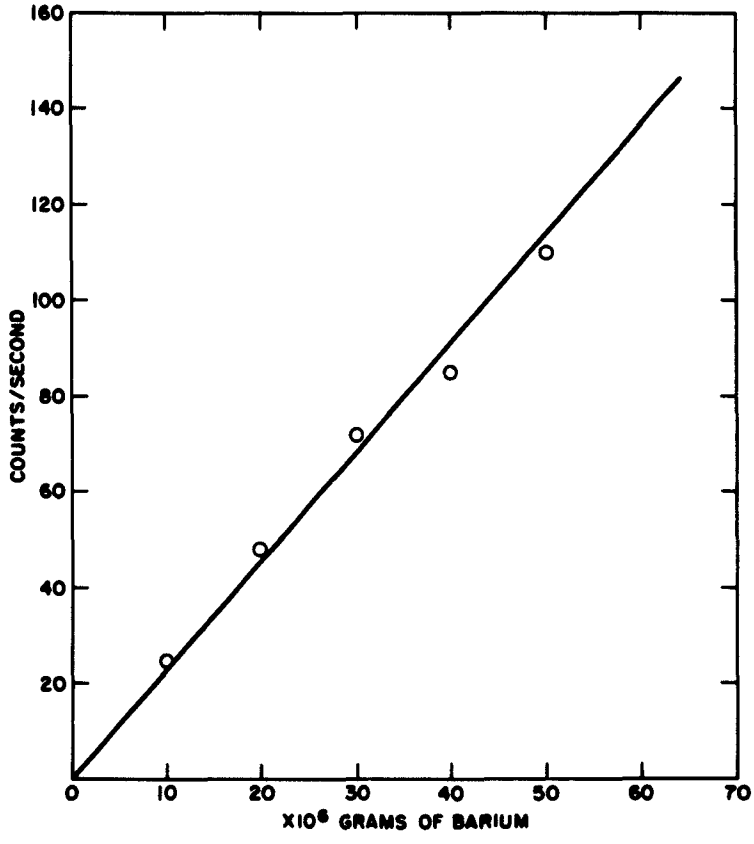

Figure 2 - Calibration Curve

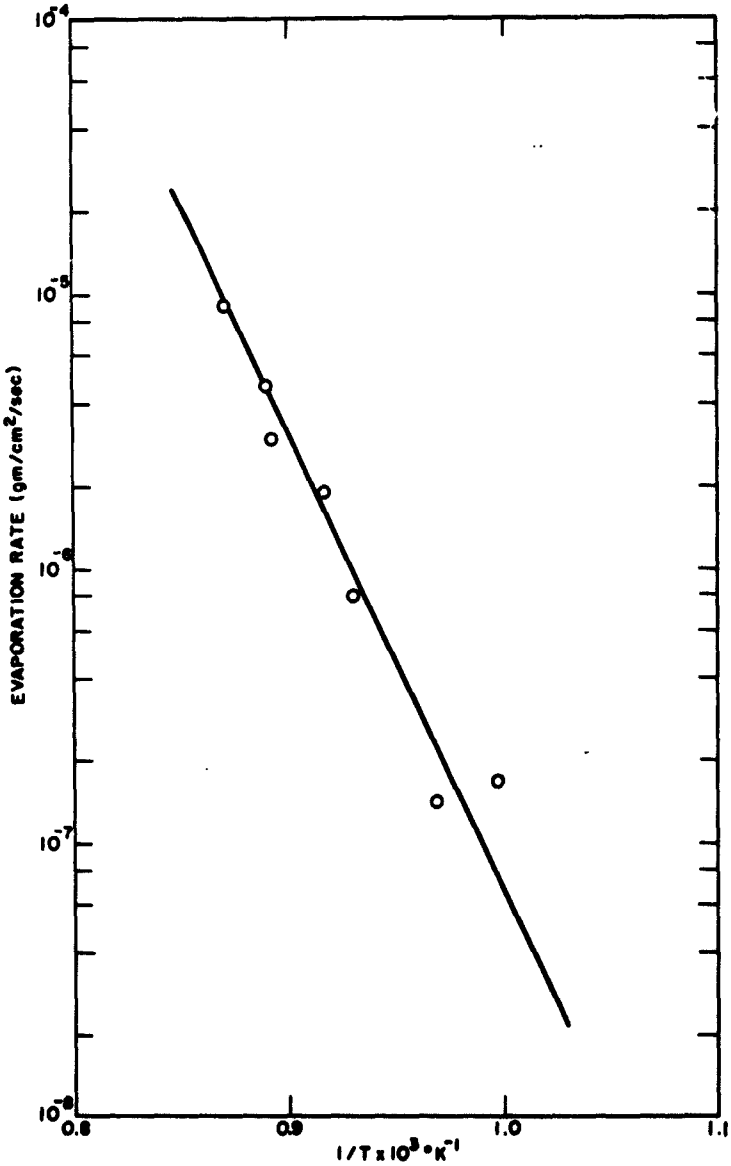

Figure 3 - Evaporation Rate of Barium from $W + BaSi_4$

$$\log W = A - B/T \qquad (2)$$

where W = gms/cm^2/sec
T = ^{o}K
A, B = constants

The curve in Figure 3 is then written mathematically as:

$$\log W = 13.3676 - \frac{21,627.3}{T} \qquad (3)$$

Having determined the constants A and B, the evaporation rate is readily determined for any given temperature.

To demonstrate the reliability of this method, the evaporation rate of a Philips impregnated type "B" cathode was measured and compared with data obtained by Gibbons, Stout and Zemany,[1] and Rittner et al.[6] These independent measurements, made by two different techniques and three different laboratories, agree within a factor of four.

This technique provides a method of quantitatively measuring micrograms and even monolayers of evaporated deposits of barium, strontium, and calcium. It may even be extended to measure the evaporation or sublimation of elements that can normally be detected in an x-ray spectrograph. It has the advantage of being able to measure simultaneously the evaporation rates of several elements.

However, only the elements are detected and no information can be obtained regarding the manner in which the element may be combined as a compound.

References

1. M. D. Gibbons, V. L. Stout, and P. D. Zemany, Bull. Amer. Phy. Soc., Ser. II, 1, No. 6279 (1956).

2. M. D. Gibbons and V. L. Stout, Bull. Amer. Phys. Soc., Series II, 3, No. 4, p. 265 (1958).

3. H. G. Pfeiffer and P. D. Zemany, Nature, p. 397 (Aug. 28, 1954).

4. H. A. Liebhafsky, H. G. Pfeiffer, and P. D. Zemany, Anal. Chem., 27, p. 1257 (1955).

5. L. Holland and W. Steckelmacher, Vacuum, II, No. 4, pp. 346-364 (1952).

6. E. S. Rittner, W. C. Rutledge, and R. H. Ahlert, Journal of App. Physics, 28, pp. 1468-1473 (1957).

LIST A

Code	Organization	No. of Copies
AF 5	AFMTC (AFMTC Tech Library-MU-135) Patrick AFB, Fla.	1
AF 18	AUL Maxwell AFB, Ala.	1
AF 32	OAR (RROS, Col. John R. Fowler) Tempo D 4th and Independence Ave., Wash 25, D. C.	1
AF 33	AFOSR, OAR (SRYP) Tempo D 4th and Independence Ave., Wash 25, D. C.	1
AF 43	ASD (ASAPRD - Dist) Wright-Patterson AFB, Ohio	1
AF 124	RADC (RAALD) Griffiss AFB, New York Attn: Documents Library	1
AF 139	AF Missile Development Center (MDGRT) Holloman AFB, New Mexico	1
AF 314	Hq. OAR (RROSP, Maj. Richard W. Nelson) Washington 25, D. C.	1
AF 318	ARL (ARA-2) Library AFL 2292, Building 450 Wright-Patterson AFB, Ohio	1
Ar 5	Commanding General USASRDL Ft. Monmouth, N. J. Attn: Tech Doc. Ctr. SIGRA/SL-ADT	1
Ar 9	Department of the Army Office of the Chief Signal Officer Washington 25, D. C. Attn: SIGRD-4a-2	1
Ar 50	Commanding Officer Attn: ORDTL-012 Diamond Ordnance Fuze Laboratories Washington 25, D. C.	1

Code	Organization	No. of Copies
Ar 67	Redstone Scientific Information Center U.S. Army Missile Command Redstone Arsenal, Alabama	1
G 31	Office of Scientific Intelligence Central Intelligence Agency 2430 E Street, N. W. Washington 25, D. C.	1
G 2	ASTIA (TIPAA) Arlington Hall Station Arlington 12, Virginia	15
G 68	Scientific and Technical Information Facility Attn: NASA Representative (S-AK/DL) P.O. Box 5700 Bethesda, Maryland	1
G 109	Director Langley Research Center National Aeronautics and Space Administration Langley Field, Virginia	1
N 9	Chief, Bureau of Naval Weapons Department of the Navy Washington 25, D. C. Attn: DLI-31	2
N 29	Director (Code 2027) U.S. Naval Research Laboratory Washington 25, D. C.	2
I 292	Director - USAF Project RAND The Rand Corporation 1700 Main Street Santa Monica, California THRU: AF Liaison Office	1
M 6	AFCRL. OAR (CRXRA - Stop 39) L. G. Hanscom Field Bedford, Massachusetts	20
AF 253	Technical Information Office European Office, Aerospace Research Shell Building, 47Cantersteen Brussels, Belgium	1

Code	Organization	No. of Copies
Ar 107	U.S. Army Aviation Human Research Unit U.S. Continental Army Command P.O. Box 428, Fort Rucker, Alabama Attn: Maj. Arne H. Eliasson	1
G 8	Library Boulder Laboratories National Bureau of Standards Boulder, Colorado	2
M 63	Institute of the Aerospace Sciences, Inc. 2 East 64th Street New York 21, New York Attn: Librarian	1
N 73	Office of Naval Research Branch Office, London Navy 100, Box 39 F.P.O., New York, N.Y.	1
U 32	Massachusetts Institute of Technology Research Laboratory Building 26, Room 327 Cambridge 39, Massachusetts Attn: John H. Hewitt	1
U 431	Alderman Library University of Virginia Charlottesville, Virginia	1
G 9	Defence Research Member Canadian Joint Staff 2450 Massachusetts Ave., N.W. Washington 25, D.C.	1
Remaining copies to:	Hq. AFCRL, OAR (CRRCPV, J. H. Bloom) L. G. Hanscom Field Bedford, Massachusetts	15

AD

General Electric Company, Power Tube Department, Schenectady, New York
INVESTIGATION OF VARIOUS ACTIVATOR REFRACTORY SUBSTRATE COMBINATIONS, by J. H. Affleck, March 5, 1963. 97 p. illus. (Proj. 4619, Task 461901 (Final Report; AFCRL-
(AF 19(628)-279) Unclassified Report

An investigation has been conducted to study thin-film activator-refractory substrate combinations to produce new materials capable of producing high emission density cathodes. Consideration is given to the nature of the boundary, the surface of the cathode, and vacuum in an externally dispensed system. Although a relation between the relative evaporation rate of electrons and the evaporation rate of the activator may be obtained, experimental confirmation in compliance with the basic assumptions is extremely difficult. An empirical examination of internally dispensed systems has been made to show what effect the substrate has on the thermionic properties of a dispenser cathode. A number of systems are reported which combine a barium compound
(over)

UNCLASSIFIED

1. Refractory substrate combinations
I. Affleck, J. H.
II. Air Force Cambridge Research Laboratories, Office of Aerospace Research
III. Contract AF 19(628)-279

UNCLASSIFIED

AD

General Electric Company, Power Tube Department, Schenectady, New York
INVESTIGATION OF VARIOUS ACTIVATOR REFRACTORY SUBSTRATE COMBINATIONS, by J. H. Affleck, March 5, 1963. 97 p. illus. (Proj. 4619, Task 461901 (Final Report; AFCRL-
(AF 19(628)-279) Unclassified Report

An investigation has been conducted to study thin-film activator-refractory substrate combinations to produce new materials capable of producing high emission density cathodes. Consideration is given to the nature of the boundary, the surface of the cathode, and vacuum in an externally dispensed system. Although a relation between the relative evaporation rate of electrons and the evaporation rate of the activator may be obtained, experimental confirmation in compliance with the basic assumptions is extremely difficult. An empirical examination of internally dispensed systems has been made to show what effect the substrate has on the thermionic properties of a dispenser cathode. A number of systems are reported which combine a barium compound
(over)

UNCLASSIFIED

1. Refractory substrate combinations
I. Affleck, J. H.
II. Air Force Cambridge Research Laboratories, Office of Aerospace Research
III. Contract AF 19(628)-279

UNCLASSIFIED

AD

General Electric Company, Power Tube Department, Schenectady, New York
INVESTIGATION OF VARIOUS ACTIVATOR REFRACTORY SUBSTRATE COMBINATIONS, by J. H. Affleck, March 5, 1963. 97 p. illus. (Proj. 4619, Task 461901 (Final Report; AFCRL-
(AF 19(628)-279) Unclassified Report

An investigation has been conducted to study thin-film activator-refractory substrate combinations to produce new materials capable of producing high emission density cathodes. Consideration is given to the nature of the boundary, the surface of the cathode, and vacuum in an externally dispensed system. Although a relation between the relative evaporation rate of electrons and the evaporation rate of the activator may be obtained, experimental confirmation in compliance with the basic assumptions is extremely difficult. An empirical examination of internally dispensed systems has been made to show what effect the substrate has on the thermionic properties of a dispenser cathode. A number of systems are reported which combine a barium compound
(over)

UNCLASSIFIED

1. Refractory substrate combinations
I. Affleck, J. H.
II. Air Force Cambridge Research Laboratories, Office of Aerospace Research
III. Contract AF 19(628)-279

UNCLASSIFIED

AD

General Electric Company, Power Tube Department, Schenectady, New York
INVESTIGATION OF VARIOUS ACTIVATOR REFRACTORY SUBSTRATE COMBINATIONS, by J. H. Affleck, March 5, 1963. 97 p. illus. (Proj. 4619, Task 461901 (Final Report. AFCRL-
(AF 19(628)-279) Unclassified Report

An investigation has been conducted to study thin-film activator-refractory substrate combinations to produce new materials capable of producing high emission density cathodes. Consideration is given to the nature of the boundary, the surface of the cathode, and vacuum in an externally dispensed system. Although a relation between the relative evaporation rate of electrons and the evaporation rate of the activator may be obtained, experimental confirmation in compliance with the basic assumptions is extremely difficult. An empirical examination of internally dispensed systems has been made to show what effect the substrate has on the thermionic properties of a dispenser cathode. A number of systems are reported which combine a barium compound
(over)

UNCLASSIFIED

1. Refractory substrate combinations
I. Affleck, J. H.
II. Air Force Cambridge Research Laboratories, Office of Aerospace Research
III. Contract AF 19(628)-279

UNCLASSIFIED

AD

with a refractory material such as tungsten, tantalum, molybdenum, or one of the carbides, borides or silicides of these same elements. As a result of the determination of the thermionic constants and the evaporation rate of the activator, it appears that the activator-substrate combination has only a secondary effect on the thermionic properties in the system examined. This is attributed to the nonuniformity of the emitting surface and to the absence of exactly a monolayer coverage by the activator.

UNCLASSIFIED

UNCLASSIFIED

AD

with a refractory material such as tungsten, tantalum, molybdenum, or one of the carbides, borides or silicides of these same elements. As a result of the determination of the thermionic constants and the evaporation rate of the activator, it appears that the activator-substrate combination has only a secondary effect on the thermionic properties in the system examined. This is attributed to the nonuniformity of the emitting surface and to the absence of exactly a monolayer coverage by the activator.

UNCLASSIFIED

UNCLASSIFIED

AD

with a refractory material such as tungsten, tantalum, molybdenum, or one of the carbides, borides or silicides of these same elements. As a result of the determination of the thermionic constants and the evaporation rate of the activator, it appears that the activator-substrate combination has only a secondary effect on the thermionic properties in the system examined. This is attributed to the nonuniformity of the emitting surface and to the absence of exactly a monolayer coverage by the activator.

UNCLASSIFIED

UNCLASSIFIED

AD

with a refractory material such as tungsten, tantalum, molybdenum, or one of the carbides, borides or silicides of these same elements. As a result of the determination of the thermionic constants and the evaporation rate of the activator, it appears that the activator-substrate combination has only a secondary effect on the thermionic properties in the system examined. This is attributed to the nonuniformity of the emitting surface and to the absence of exactly a monolayer coverage by the activator.

UNCLASSIFIED

UNCLASSIFIED